Experiments and Computational Modeling of Pulverized Coal Ignition

FINAL REPORT

Reporting Period Start Date: 10/01/1996 End Date: 09/30/1999

Authors:
Samuel Owusu-Ofori
John C. Chen (Rowan University)

Report Issue Date: 12/31/1999

DE-FG22-96PC96221--06

North Carolina A&T State University
1601 East Market Street
Greensboro, NC 27411

Rowan University
201 Mullica Hill Road
Glassboro, NJ 08028

DISCLAIMER

ABSTRACT

Under typical conditions of pulverized-coal combustion, which is characterized by fine particles heated at very high rates, there is currently a lack of certainty regarding the ignition mechanism of bituminous and lower rank coals as well as the ignition rate of reaction. Furthermore, there have been no previous studies aimed at examining these factors under various experimental conditions, such as particle size, oxygen concentration, and heating rate. Finally, there is a need to improve current mathematical models of ignition to realistically and accurately depict the particle-to-particle variations that exist within a coal sample. Such a model is needed to extract useful reaction parameters from ignition studies, and to interpret ignition data in a more meaningful way.

We propose to examine fundamental aspects of coal ignition through (1) experiments to determine the ignition temperature of various coals by direct measurement, and (2) modeling of the ignition process to derive rate constants and to provide a more insightful interpretation of data from ignition experiments.

We propose to use a novel laser-based ignition experiment to achieve our first objective. Laser-ignition experiments offer the distinct advantage of easy optical access to the particles because of the absence of a furnace or radiating walls, and thus permit direct observation and particle temperature measurement. The ignition temperature of different coals under various experimental conditions can therefore be easily determined by direct measurement using two-color pyrometry. The ignition rate-constants, when the ignition occurs heterogeneously, and the particle heating rates will both be determined from analyses based on these measurements.

For the modeling portion of this study we will complete the development of the Distributed Activation Energy Model of Ignition (DAEMI), which simulates the conventional drop-tube furnace ignition experiment. The DAEMI accounts for particle-to-particle variations in reactivity by having a single preexponential factor and a Gaussian distribution of activation energies among the particles. Previous results show that the model captures the key experimental observations, and that adjustments to the model parameters permit a good fit to experimental data. We will complete the model by (1) examining the effects of other variations in physical parameters on the model, (2) applying the model to published results in order to extract reaction parameters, and (3) extending the model for application to laser-based ignition studies, such as our own.

TABLE OF CONTENTS

EXECUTIVE SUMMARY

Under typical conditions of pulverized-coal combustion, which is characterized by fine particles heated at very high rates, there is currently a lack of certainty regarding the ignition mechanism of bituminous and lower rank coals as well as the ignition rate of reaction. Furthermore, there have been no previous studies aimed at examining these factors under various experimental conditions, such as particle size, oxygen concentration, and heating rate. Finally, there is a need to improve current mathematical models of ignition to realistically and accurately depict the particle-to-particle variations that exist within a coal sample. Such a model is needed to extract useful reaction parameters from ignition studies, and to interpret ignition data in a more meaningful way.

In this project, we investigated fundamental aspects of coal ignition through (1) experiments to determine the ignition temperature of various coals by direct measurement, and (2) modeling of the ignition process to derive rate constants and to provide a more insightful interpretation of data from ignition experiments.

The specific objectives of this project were:

1. develop a novel experimental facility with extensive optical-diagnostic capabilities to study coal ignition;
2. determine the ignition temperature of coals under simulated combustion conditions by direct measurement with two-color pyrometry;
3. examine the effects of various experimental conditions, including coal rank, particle size, oxygen concentration and heating rate, on the ignition temperature;
4. determine the ignition rate constants of various coals.
5. modify our existing ignition model to examine the effect of particle-size distribution on the ignition behavior;
6. incorporate, if necessary, a size distribution into the model;
7. apply the model to extract ignition rate constants from previously published data from conventional experiments;
8. modify the model and apply it to our laser-based ignition studies for determination of ignition rate constants.

All of the project objectives were achieved in the period of this grant. Some specific findings from this project are:

1. ignition temperatures measured using our laser-ignition experiment showed a wide range of values, due most likely to the wide distribution of reactivity among coal particles within a sample;
2. there is no apparent relation between coal rank and reactivity distribution, as determined by our model of ignition (DAEMI);
3. ignition temperatures were highest for the Pittsburgh #8, high-volatile bituminous coal and was lower for both the Pust lignite and Wyodak subbituminous coal, both of which showed similar ignition temperatures;
4. based on #3 above, it is concluded that the ignition reactivity is highest for the high-volatile bituminous coal, and is lower for the lignite and subbituminous coals, consistent with the combustion reactivity of these coal types;
5. the DAEMI base case showed that the results are sensitive to the number of particles (M) considered in the model, as expected;
6. the DAEMI base case showed that the model is insensitive to the particle size distribution, as a top-hat distribution gave similar results to that found using a constant particle size;
7. the DAEMI, although capable of capturing the behavior of the laser-ignition experiment, could not be adjusted to accurately model the results, due most likely to the wide range of ignition temperatures measured;
8. the DAEMI accurately modeled the results from a conventional drop-tube furnace experiment based on two coals and a wide range of particle sizes and oxygen concentration, and was successful in extracting the ignition rate constants.

INTRODUCTION

The ignition of pulverized coal has been the subject of research for nearly 150 years, with the initial motivation being the avoidance of coal-dust explosions in mines. In more recent times, due to the world's increased reliance on coal for power generation and the need to maximize energy-conversion efficiency, research has shifted to understanding the fundamental mechanism of coal ignition and measuring its kinetic rates. The importance of ignition to coal-flame stability is obvious — the more easily a particular coal ignites after injection into a boiler furnace, the better its flame-stability characteristics. A less obvious ramification of the ignition process is its role in establishing extended, fuel-rich zones in coal flames which are responsible for the destruction of NO_x and its conversion to benign N2. Certainly, the ignition process is inextricably linked to the formation of this NO_x-reduction zone, and the ignition behavior of coals and coal blends will strongly affect the ease and extent of formation of this zone. This connection is deserving of further study and its understanding is the goal toward which we hope to apply the results of this proposed study. Specifically, we propose to examine fundamental aspects of coal ignition through (1) experiments to elucidate the ignition behavior of coals and to measure the ignition temperature, and (2) modeling of the process to derive accurate and useful rate constants and to provide a more insightful interpretation of data from ignition experiments.

PROJECT OBJECTIVES

Our objectives for this project are to:

1. develop a novel experimental facility with extensive optical-diagnostic capabilities to study coal ignition;
2. determine the ignition temperature of coals under simulated combustion conditions by direct measurement with two-color pyrometry;
3. examine the effects of various experimental conditions, including coal rank, particle size, oxygen concentration and heating rate, on the ignition temperature;
4. determine the ignition rate constants of various coals.
5. modify our existing ignition model to examine the effect of particle-size distribution on the ignition behavior;
6. incorporate, if necessary, a size distribution into the model;

7. apply the model to extract ignition rate constants from previously published data from conventional experiments;
8. modify the model and apply it to our laser-based ignition studies for determination of ignition rate constants.

RESULTS AND DISCUSSION

1. Personnel

This project has supported numerous undergraduate and graduate students during its period of activity. In all, five undergraduate students actively participated in various aspects of this project and two graduate students played a major role in its completion. Both graduate students (Ms. Jianping Zheng and Ms. Vida Ohene-Agyeman) received their Master of Science degree based on their work on this project.

2. Experimental Set-up

Overview

A schematic diagram of the experiment is presented in Figure 2.1. Sieve-sized coals are dropped, batch-wise, into a laminar upward-flow wind tunnel with a quartz test section. The gas is not preheated, and this allows for a direct optical observation of ignition sequence. The uniform gas velocity is adjusted to be greater than the particle terminal velocity so that the particle emerges from the feeder tube, falls approximately 5 cm, and then travels upward out of the tunnel. This ensures that the particles move slowly downward at the ignition point, chosen to be 3.0 cm below the feeder-tube exit.

A single pulse from a Nd: YAG laser is directed to heat the coal particles by focusing the beam and deflecting it at an angle through the test section. The beam is then defocused upon exiting the test section. Two additional prisms fold the beam back through the ignition point and this achieves spatial uniformity in heating the coal particles in that the coal particles are heated on two sides. Heating the coal particles in such a manner allows for higher energy input than a single laser pass. For nearly every case, two to five particles are contained in the volume formed by the two intersecting beams, as observed using the high-speed video.

A small aluminum block mounted on air-driven piston is used as a gate to permit the passage of the single laser pulse. The gate is either open or closed by applying pressure on the air chambers on both sides of the piston. The airflow to the chambers is controlled using an

electronic valve whilst a digital pulse generator is employed for accurate timing. This system allows for the control of the delay time between the firing of the feeder and the passage of the laser pulse, which is necessary since coal samples of different sizes and/or densities required different time periods to fall through the feeder tube. A polarizer placed outside of the laser head varies the pulsed radiation delivered to the test section and variation from 150 –750mJ per pulse is achieved using this polarizer. Finally, ignition or non-ignition is determined by examining the signal generated by a high-speed silicon photodiode connected to a digital oscilloscope.

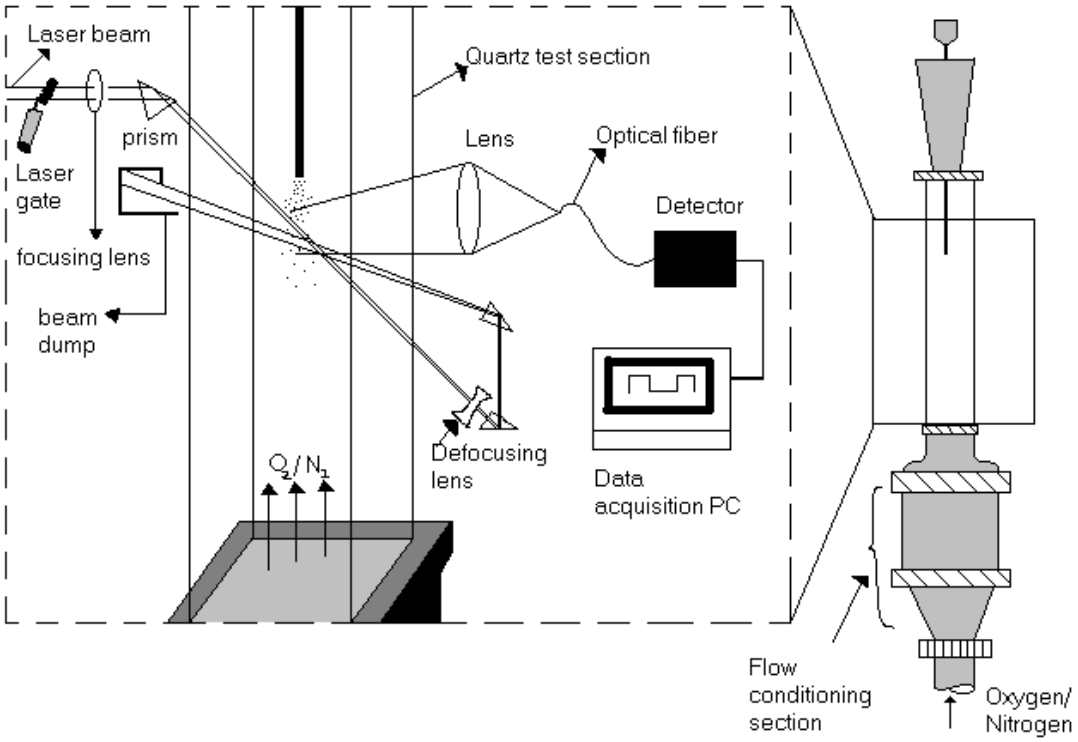

Figure 2.1. Schematic of the laser ignition apparatus

Coal Preparation

Coals were received from Penn State Coal Sample Bank packed under an argon atmosphere. Approximately 150g of coal was transferred into pint jars for vacuum drying at 10 in. Hg and 76°C for 8 hours. Each sample is then dry-sieved, stored in 16-oz jars, and kept in dessicator cabinets.

Samples in the amount of about 50g are sieved in a single pass using a Ro-Tap sieve shaker. Table 2.1 below shows a list of mesh numbers and their corresponding opening

diameters for the sieves used. Since the shaker did not accommodate all eight sieves at a time, the sieving was done in two batches. The first four sieves used were sizes 80, 100, 120 and 140 meshes with 80 mesh size at the top and 140 mesh size at the bottom. The sieves were shaken for fifteen minutes and the underside of each sieve is vacuum suctioned for about a minute to remove all fine particles that could possibly be attached to the sieve. The particles on each mesh were then emptied into small bottles for storage. A small brush was used to gently remove any particles, which lodged in the mesh that could not be removed by suction. The remaining sample, which passed through the 140-mesh sieve, was the starting sample for the second set of sieves with 170 mesh at the top and 270 at the bottom. The same procedure was repeated for this set of sieves.

The coals collected were in the following mesh sizes: -80/+100, -100/+120, -120/+140, -140/+170, -170/+200, -200/+230, and –230/+270. The +80 and –270 mesh samples were not used because they were not size–classified. Three different coal samples ranging in rank from lignites to low volatile bituminous were prepared in the same manner as described and then stored for use. Table 2.2 shows the different types of coals and their compositions that were used.

Table 2.1. Mesh sizes and their respective size ranges

Mesh	Size range of particles retained (μm)
+80	180 and above
+100	150 – 180
+120	125 – 150
+140	106 – 125
+170	90 – 106
+200	75 – 90
+230	63 –75
+270	53 – 63

Table 2.2. Proximate and Ultimate Analysis of Coal Samples

	Dry wt%		Dry, Ash-free wt%			
Coal Type	Volatile Matter	Ash Content	C	H	N	O + S (diff)
DECS 23 Pittsburgh High volatile bituminous	39.42	9.44	74.21	5.10	1.35	9.90
DECS 25 Pust Lignite A	41.98	11.85	65.76	4.60	0.94	16.85
DECS 26 Wyodak Sub-bituminous	44.86	7.59	69.77	5.65	0.94	16.07

Gas Flow System

The gas flow system is shown in Figure 2.2. Oxygen and nitrogen are supplied to the wind tunnel by directing them through flowmeters and pressure regulators. The two gases are either blended in the required ratio and flow rates to obtain a mixture or pure oxygen in the required flow rate is directed to the wind tunnel through an aluminum tube.

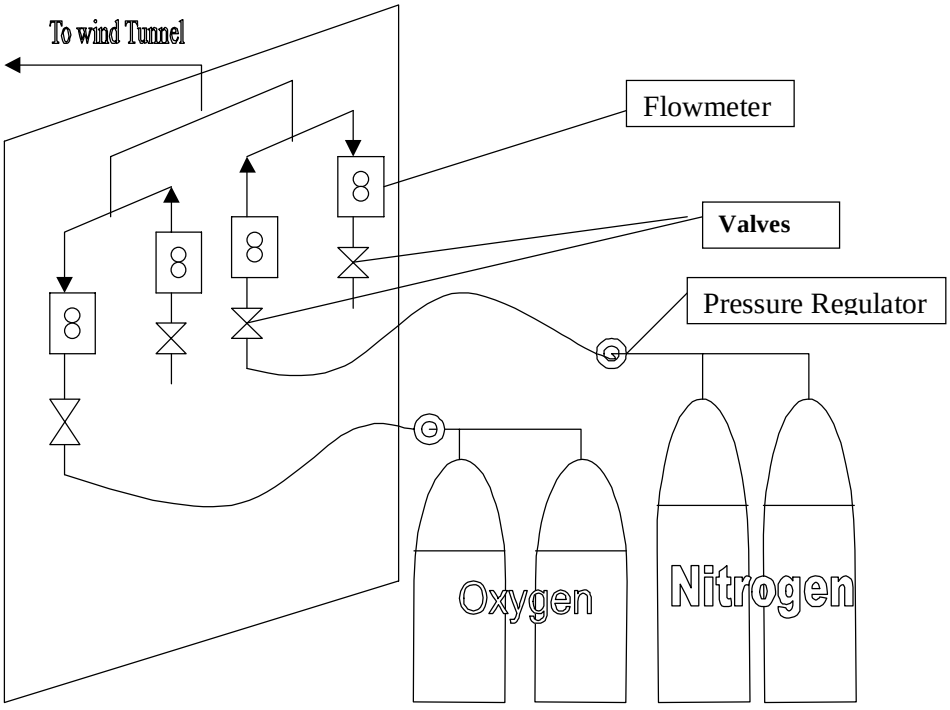

Figure 2.2. Schematic showing gas-handling system.

Wind Tunnel

This is constructed of the following: a 90° elbow, a wide-angle diffuser, two wire meshes and a honeycomb. As shown in Figure 2.3, the initial elbow with a cross section of 57 mm is followed by the wide-angle diffuser that has a square cross-section of 122 mm and this expands the flow into the flow-conditioning section. The two wire meshes and honeycomb are used in the flow conditioner to reduce turbulence and to straighten the flow. A honeycomb upstream of the test section ensured flow uniformity for some distance downstream. The gas stream is then directed to the transparent test section through a contraction section to prevent the coal particles from falling below the ignition point depth. This gas stream passing through the quartz section leaves the wind tunnel through the diffuser along with the coal particles that could not be ignited.

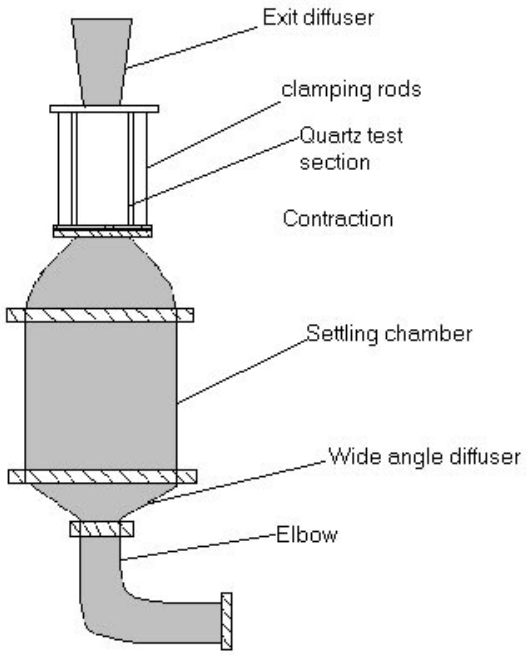

Figure 2.3. Schematic showing the wind tunnel layout

Feeder

Figure 2.4 shows a schematic of the feeder. It comprises a capped cylinder (12 mm ID) with a tapered bottom connected to a 4-mm tube. A wire mesh is suspended within the feeder and this supports a mound of particles. A jolt to the feeder results in particles falling through the mesh and into the feeder tube. A small air-driven piston, controlled electronically through

solenoid valve, hits the feeder at each pulse to provide the required jolt. In order to allow only a few particles to fall through the mesh at each jolt, the mesh used had a size larger than the finest through which the particles could pass. Table 2.3 provides a list of meshes used for our experiments.

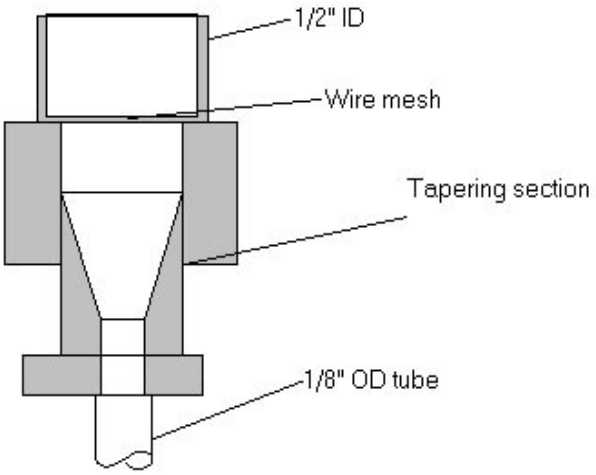

Figure 2.4. Cross-sectional view of the coal feeder.

Table 2.3. Mesh used for feeder

Particle Size(μm)	Mesh used
150 – 180	60
106 – 125	80
63 – 75	100

Laser and Optical System

The laser used is a Nd:YAG laser that operates at a pulse rate of 10 Hz with a pulse duration of 100 μs. The pulse energy emerging directly from the laser is set at 850 mJ per pulse in the primary (1064 nm) output with a pulse-to-pulse energy fluctuation of 3%. The required laser pulse energy delivered is achieved by rotating a polarizer which is located at the distance outside the laser head. At the ignition point, the beam diameter normal to its direction of propagation is approximately 2.5 mm on each pass. The laser is triggered externally by the digital pulse generator; a second pulse is synchronized with the first generator to control the delay time between firing of the feeder and the laser gate, which determines the delay in the passage of the laser pulse through the test section.

The laser beam is focused through the tunnel using a convex lens (focal length 750mm). It is defocused upon leaving the test section using a concave lens (focal length 150 mm). The defocused beam is then folded back to the ignition point and finally stopped by a beam dump. This is presented in Figure 2.1.

Detector and Pyrometry System

Figure 2.5 shows a schematic of the detector and pyrometry system. This consists of simple lens that collects light from the igniting particles and directs it to a fast response Si photodetector through an optical fiber bundle. The captured light from the igniting particle is split using a dichroic beamsplitter and a collection of lenses. The detector is connected to a Nicolet data acquisition computer, which records the signals. This pyrometry system is calibrated before every experimental run using a blackbody source.

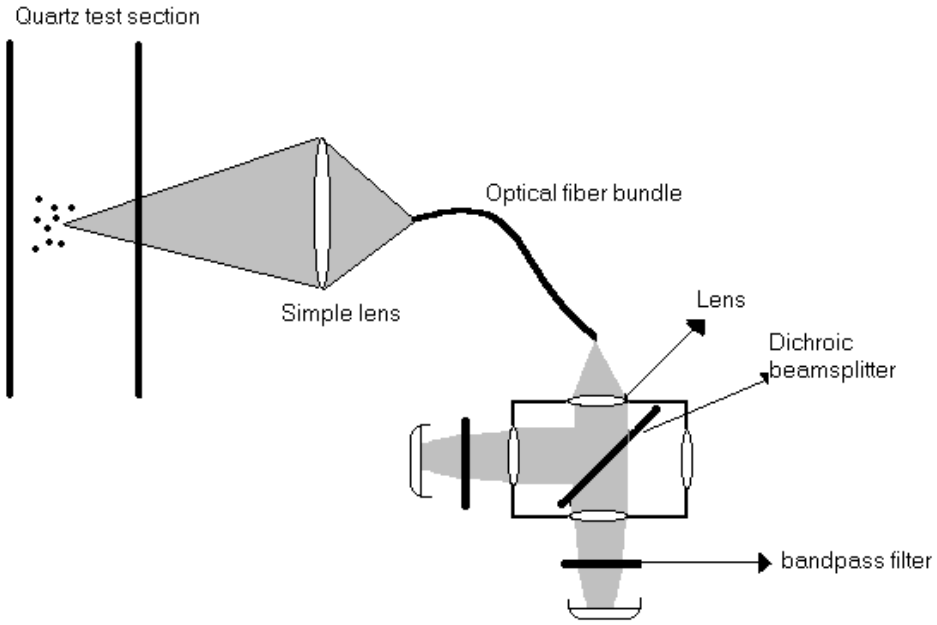

Figure 2.5. Schematic of the detector and optical system

Blackbody

To calibrate the pyrometry system, the blackbody is set to a temperature of about 990°C. At this temperature, light emitted from this source is directed towards the detector and pyrometry system and the signal is then recorded using the Nicolet acquisition system. The

light emitted is pulsed using a small piece of hard paper to block the simple lens collecting the light intermittently.

Ignition Signal

A typical set of data and observed signals are shown in the following figures. An ignition signal is characterized by the sharp spark as shown in Figure 2.6a. In this instance the energy absorbed is concentrated on the surface of the particle and this energy is conducted internally with time.

The signal for the spark represents the energy recorded on the surface of the particle. As the energy is distributed evenly, that on the surface is lowered and hence the signal recorded drops sharply. If there is enough energy to initiate ignition after the drop, ignition occurs and more energy is generated resulting in the rise of the signal again. Hence Figure 2.6b shows ignition with multiple peaks before finally decreasing to the zero line.

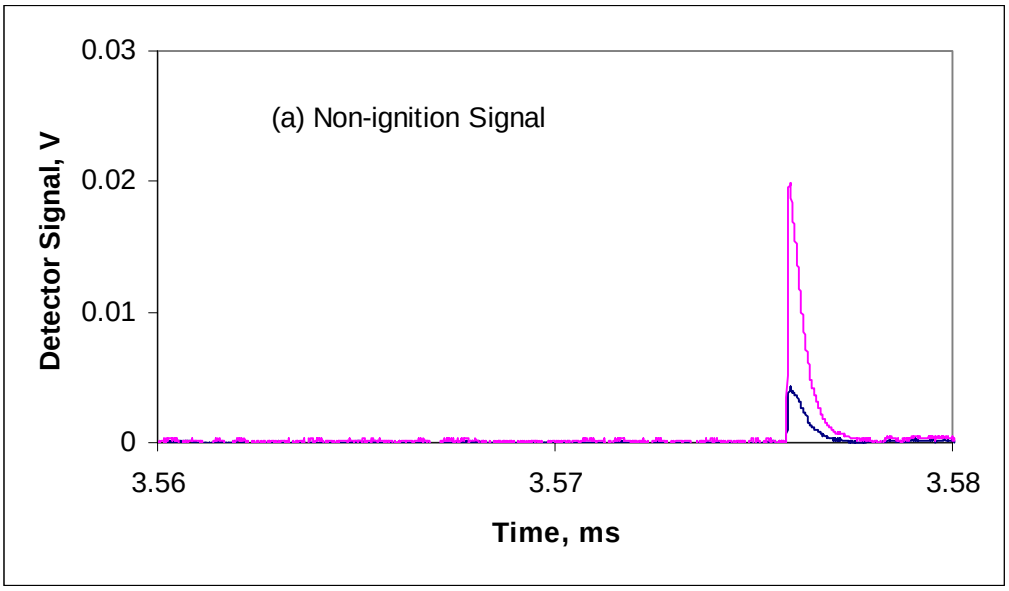

Figure 2.6a. Signal traces from photodetectors showing non-ignition for Wyodak coal.

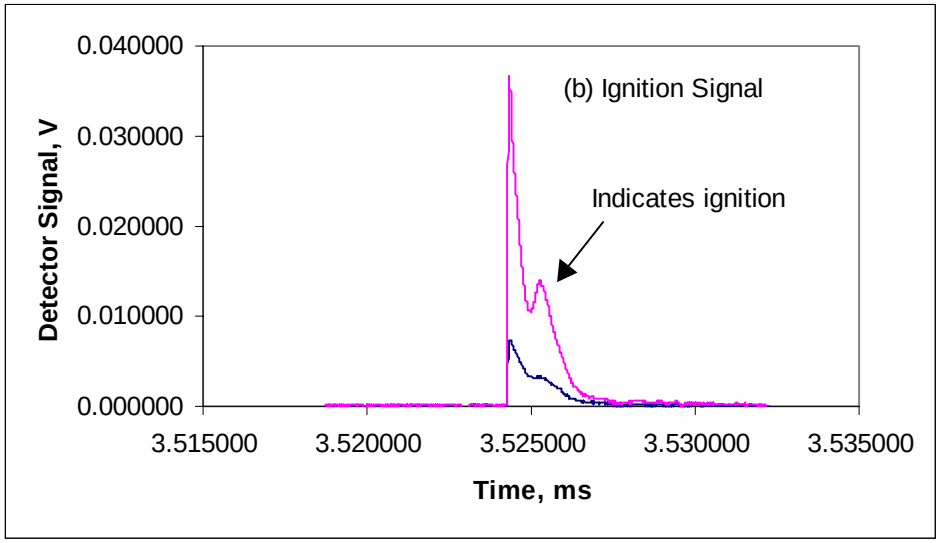

Figure 2.6b. Signal traces from photodetectors showing ignition for Wyodak coal.

3. Experimental Results

The experiment provides data of ignition frequency for various oxygen concentrations, particle diameter and coal type. Two sizes of three types of coals under two oxygen concentrations have been examined. At each set of conditions, the ignition frequency, or probability of ignition was measured over a range of laser pulse energy values. The ignition temperatures for all the coal types under the set conditions were also measured from the signals.

Ignition-Frequency Distribution Data

The experimental results were translated in order to explain and draw conclusions from the observations. The tables shown represent the translations obtained. In each table, we have the coal type, the particle size, polarizer angle and its corresponding laser energy, and the frequencies in terms of percentages for each experimental run. The ignition frequency is obtained from the number of ignitions obtained out of 20 experimental runs for each condition considered. The energy values were obtained from measurements relating the polarizer angle to the laser energy values. The frequencies thus obtained were mapped against the corresponding laser energies for these coals as ignition-frequency distributions.

Table 3.1. Experimental data for Wyodak coal

Size (μm)	Oxygen Concentration (%)	Polarizer angle, °	Laser Energy Pulse, mJ	Frequency (%)
150-180	100	302	220	45
		305	280	45
		310	340	75
		315	400	100
150-180	67	310	340	20
		315	400	50
		320	455	60
		325	515	70
106-125	100	300	240	20
		305	280	50
		310	340	70
		315	400	90
106-125	67	307	302.5	35
		310	340	60
		315	400	40
		325	515	90

Table 3.2. Experimental data for Pust coal

Size (μm)	Oxygen Concentration (%)	Polarizer angle, °	Laser Energy Pulse, mJ	Frequency (%)
150-180	100	300	220	25
		305	280	35
		310	340	60
		313	375	80
		318	432.5	90
150-180	67	310	340	15
		315	400	25
		320	455	35
		325	515	55
		330	570	65
106-125	100	295	170	15
		298	200	30
		300	220	60
		305	280	80
106-125	67	305	280	35
		310	340	55
		315	400	70
		320	455	100

Table 3.3. Experimental data for Pittsburgh #8 coal

Size (μm)	Oxygen Concentration (%)	Polarizer angle, °	Laser Energy Pulse, mJ	Frequency (%)
150-180	100	300	220	30
		305	280	65
		310	340	75
150-180	67	310	340	15
		315	400	25
		320	455	35
		325	515	55
		330	570	65
106-125	100	302	240	30
		305	280	50
		310	340	70
		315	400	100
106-125	67	302	240	10
		305	280	35
		307	302.5	30
		310	340	85

Figures 3.1 and 3.2 show the ignition-frequency distribution for the 106-125 μm and 150-180 μm high volatile bituminous Pittsburgh #8 coals respectively at various oxygen concentrations. It can be seen that at each oxygen concentration, the ignition frequency increases approximately linearly over a range of laser pulse energy. At each oxygen concentration, there is a lower energy below which the ignition probability is zero and a higher energy above which there is 100% ignition probability. The ignition frequency increases with increasing laser pulse energy since high pulse energy translates to a higher particle temperature. Thus, whenever the laser pulse energy is used to heat several randomly chosen particles from a batch of particles dropped into the experiment, there is an increasing probability that one of the heated particles will ignite as the particles are heated to higher temperatures.

The shifting of the distributions to higher laser energies as oxygen concentration is decreased is expected, since at lower oxygen levels, the amount of heat generated by the particle is decreased. Thus, in order to achieve a constant ignition frequency as oxygen concentration is decreased, the particles must be heated initially to a higher temperature using higher laser energy.

The general observations described apply to all coals studied and these characteristics are shown by Figures 3.3, 3.4, 3.5, and 3.6 representing ignition frequency distribution for Wyodak and Pust coals respectively in their various coal size distributions.

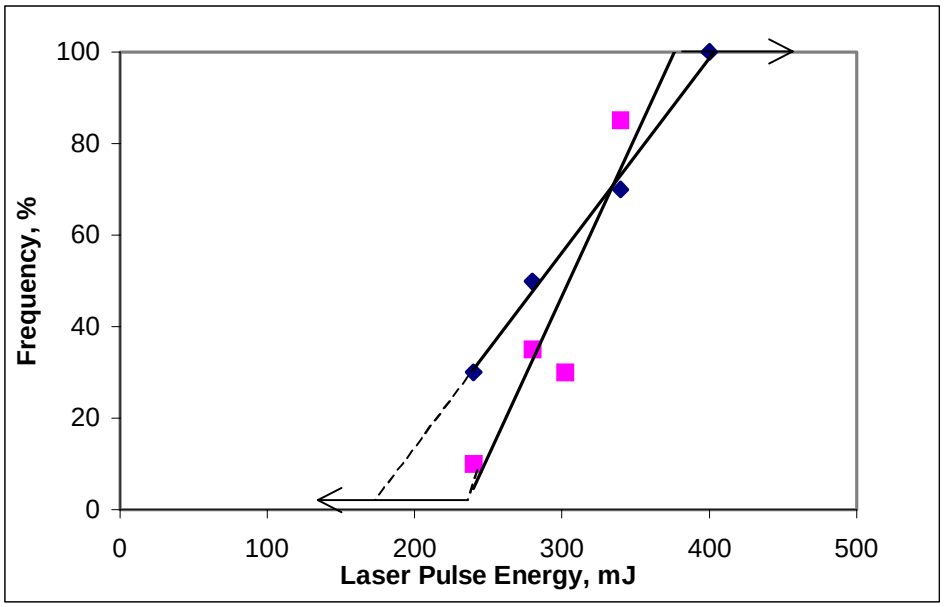

Figure 3.1. Ignition frequency distribution for Pittsburgh #8 high volatile bituminous Coal. (■) 106-125 µm particles in 100% Oxygen (♦)106-125 µm particles in 67% Oxygen.

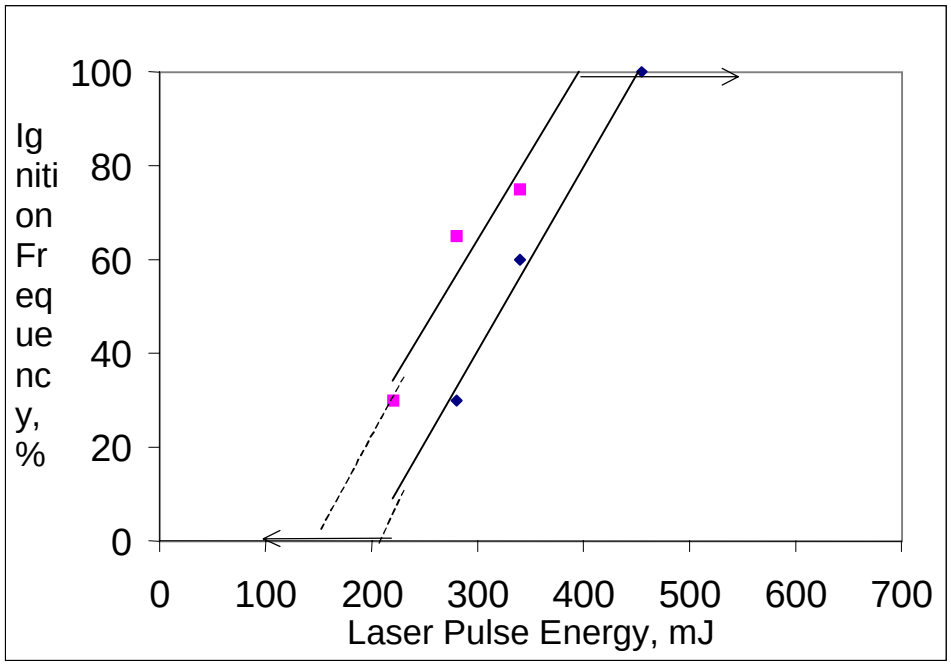

Figure 3.2. Ignition-frequency distribution for Pittsburgh #8 high volatile bituminous coal. (■) 150-180 µm particles in 100% Oxygen (▲)150-180 µm particles in 67% Oxygen.

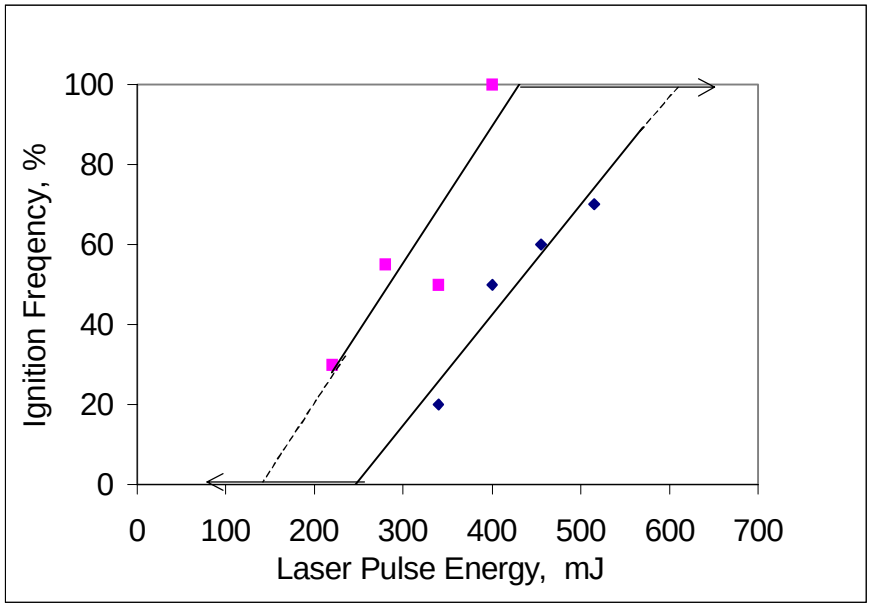

Figure 3.3. Ignition frequency distribution for Wyodak coal. (■) 106-125 μm particles in 100% Oxygen (♦) 106-125 μm particles in 67% Oxygen.

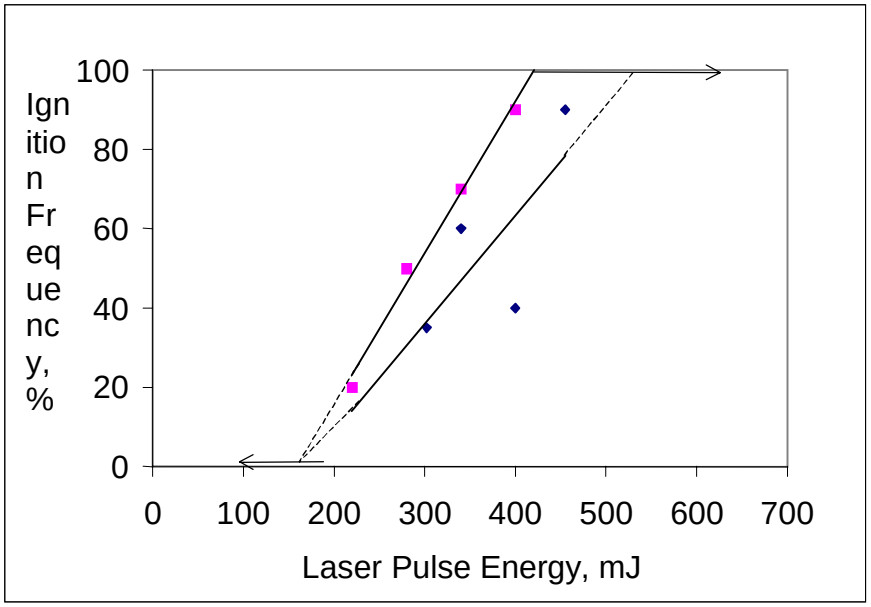

Figure 3.4. Ignition frequency distribution for Wyodak coal. (■) 150-180 μm particles in 100% Oxygen (♦) 150-180 μm particles in 67% Oxygen.

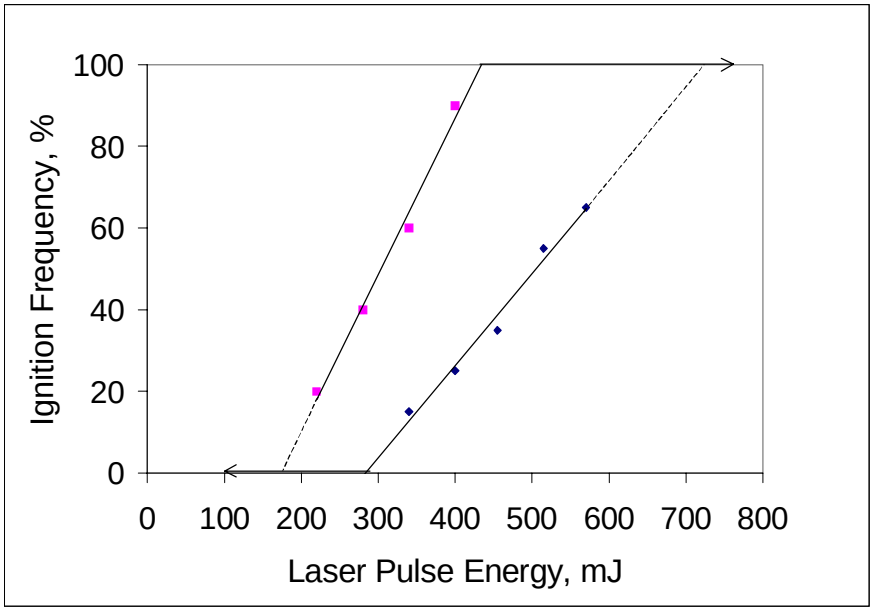

Figure 3.5. Ignition frequency distribution for Pust Lignite coal. (■) 106-125 µm particles in 100% Oxygen (♦) 106-125 µm particles in 67% Oxygen.

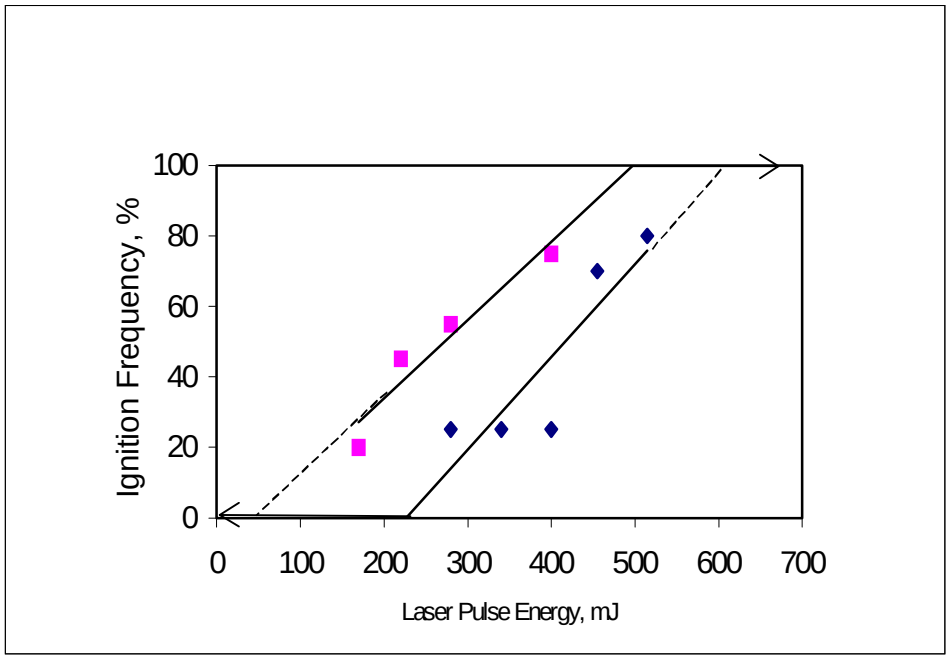

Figure 3.6. Ignition frequency distribution for Pust Lignite coal. (□) 150-180 µm particles in 100% Oxygen (♦) 150-180 µm particles in 67% Oxygen.

From the Figures shown, it can be seen that as the particle size decreases, the range of laser energy needed to span 0 to 100% ignition frequency becomes narrower; that is the slope of the ignition distribution at a given oxygen concentration is more vertical.

The range of 0-100% ignition frequency for Wyodak coals span between 200 and 400 mJ for 100 % Oxygen concentration, that for Pust is between 200 and 450 mJ whilst that for Pittsburgh #8 is between 200 and 350 mJ. Specific differences as such is due to the variations in the reactivity distributions of the coals.

The regression fits for the data are presented in Table 3.4. This table shows the coal type, the corresponding particle size, the oxygen concentration, the slopes obtained in the regression fits and the range within which they are obtained.

Table 3.4. Regression fit for data

Coal Type	Particle Size, μm	Oxygen Concentration, %	Slope	Range of Laser Energies
Pittsburgh #8	106 – 125	75	0.6994	250 – 350
		100	0.4252	250 – 400
	150 – 180	67	0.3930	250 – 425
		100	0.3750	200 – 350
Wyodak	106 – 125	67	0.2748	300 – 450
		100	0.3833	200 – 450
	150 – 180	67	0.2764	300 – 500
		100	0.3417	225 – 400
Pust	106 – 125	67	0.2629	250 – 500
		100	0.2218	180 – 450
	150 – 180	67	0.2262	300 – 575
		100	0.3833	200 – 400

Ignition Temperature Measurements

The ignition temperatures measured for all the coal samples are presented in the tables shown. The size ranges of 150-180 μm of the three coal types were considered for the temperature measurement. The table comprises the measured ignition temperatures and the corresponding laser energies at which the coals ignite. Each table represents the translated experimental data for each coal type and under all the conditions that they have been set to operate. The different temperatures measured for each laser energy are those obtained from the ignition frequency data. The ignition temperature measured is then mapped against its corresponding laser energy pulse.

Table 3.5. Laser energy and corresponding Ignition temperatures for Pust coal.

Laser energy, mJ	220	280	340	375	432.5
Ignition temperature, K **(100% Oxygen concentration)**	1699.1 2241.5	1595.2 1857.3	1830.8 1802.8	1383.8 1956 1773.8	1568.8 1611.3 1633.8 1105.5 1949.5 1815.7 2133 1944.2 1836.6
Laser energy, mJ	400	455	515	570	
Ignition temperature, K **(67% Oxygen concentration)**	1318.2 1604 1530 1410	1608.3 1579.8 1510.1 1511 1352.9	1723.6 1502.3 1723.2 1107.7 1114.4 1289.5 1546.8	1159.4 1247 1357	

Table 3.6. Laser energy and corresponding Ignition temperatures for Wyodak coal

Laser energy, (mJ)	240	280	340	400	455	515
Ignition temperature, K **(100% Oxygen concentration**)	1207.1 1573	1424.8 2087.7 1504.2 1813.1 1718.4 2107.1 1117.9	1816.5 1703 1700.9 1701.8 1414.2 1156.9 1658.4 1776.1	1273.2 1587 946.9 1602.5 2220.7 1480.9	1962 1245.3 1783.6 1527.8 1446.4	N/A
Ignition temperature, K **(67% Oxygen concentration)**	N/A	N/A	1917.6	1679.6 2006.0 1882.2 2255.2 3132.7 2144.2 2152.8 1779.3 1725.0	2816.6 2203.4 1882.2 2229.9 1885.2 2144.2 1942.7 1738.6 1924.9	1538.4 1557.8 1825.7 1687.5 1814.7 1560.0 1318.2 1861.4 2082.5 2104.2 1763.0 2139.1

Table 3.7. Laser energy and corresponding Ignition temperatures for Pittsburgh #8 coal.

Laser energy, (mJ)	220	280	340	455
Ignition temperature, K **(100% Oxygen concentration)**	2569.6 2759.0 2631.8 2805.9 2746.5 2827.7	2642.3 2573.8 2835.1 2673.2 2669.8 2506.9 2565.1 2667.8 2773.5 2405.9 2334.3 2674.0	2705.6 2711.4 2660.7 2768.3 2391.4 2656.1 2816.1 2574.3 1970.1 2688.7 2785.5 2481.7 2746.9 2496.9	N/A
Ignition temperature, K **(67% Oxygen concentration)**	N/A	2534.3 2565.0 2469.9 1912.6 2637.2	2453.0 2451.8 2362.4 2389.1 2413.0 2240.7 2579.5 2450.6 2630.6 2470.2 2429.8 2385.2	2329.3 2503.6 2616.5 2507.8 2484.8 2490.8 2576.8 2394.2 2537.4 2447.4

Figures 3.7, 3.8 and 3.9 show the ignition temperature distribution for all the three coals in their 100% and 67% Oxygen concentration. The range of the particle temperature distribution shifts to higher laser energies for lower oxygen concentration. This is expected because at lower oxygen levels, the amount of heat generated by the particle is decreased. The particles are therefore heated initially to a higher temperature using higher laser energy for ignition to occur. This results in the shift of the distribution to such higher laser energies.

It is observed that the measured temperatures for 100% oxygen concentration are higher than that for 67% oxygen concentration for Pust and Pittsburgh #8 coals. However, Wyodak behaved differently in that the measured temperatures for 67% oxygen concentration are higher than that for 100% oxygen concentration. The measured minimum particle temperatures of Pust and Wyodak coals are lower than that of Pittsburgh #8 coal. This can be attributed to the volatile matter content of the coals. Pittsburgh #8 has the lowest volatile matter content, followed by Pust and Wyodak has the highest. The coal with the highest

matter content is observed to have the lowest measured particle ignition temperatures and that with the lowest volatile matter content which is Pittsburgh #8 has the highest measured particle ignition temperature. This portrays an inverse relation between the volatile matter content and the measured particle ignition temperature. Differences observed in distributions between the coal types are attributed to the variations in the reactivity distributions of the coals.

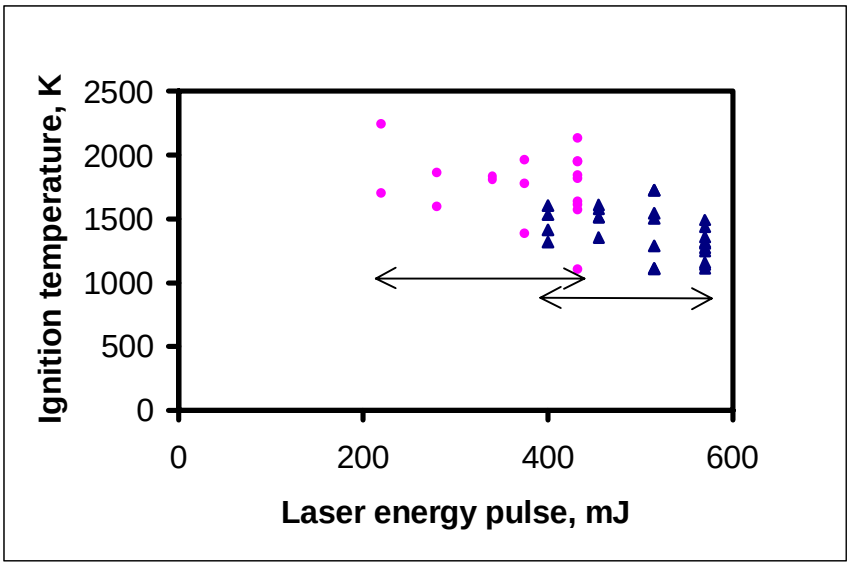

Figure 3.7. Distribution of ignition temperature against laser energy for Pust coal.

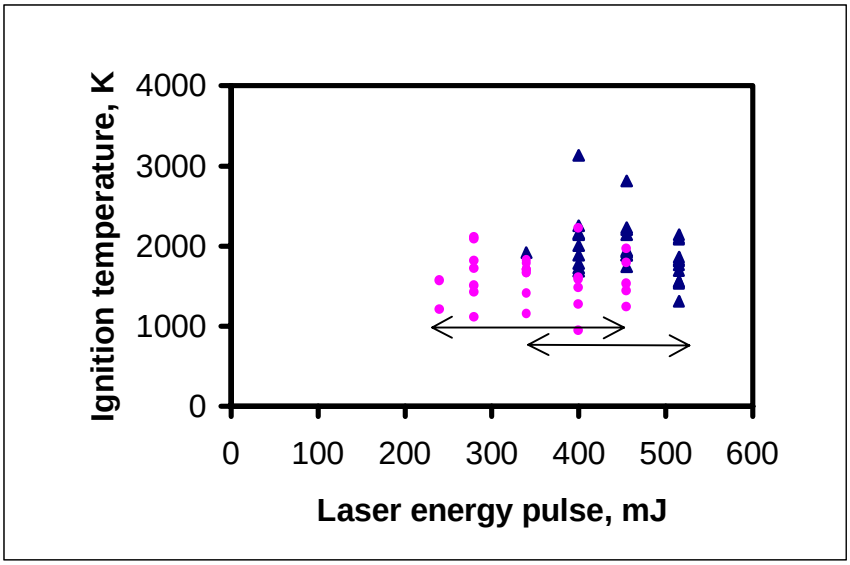

Figure 3.8. Distribution of ignition temperature against laser energy for Wyodak coal.

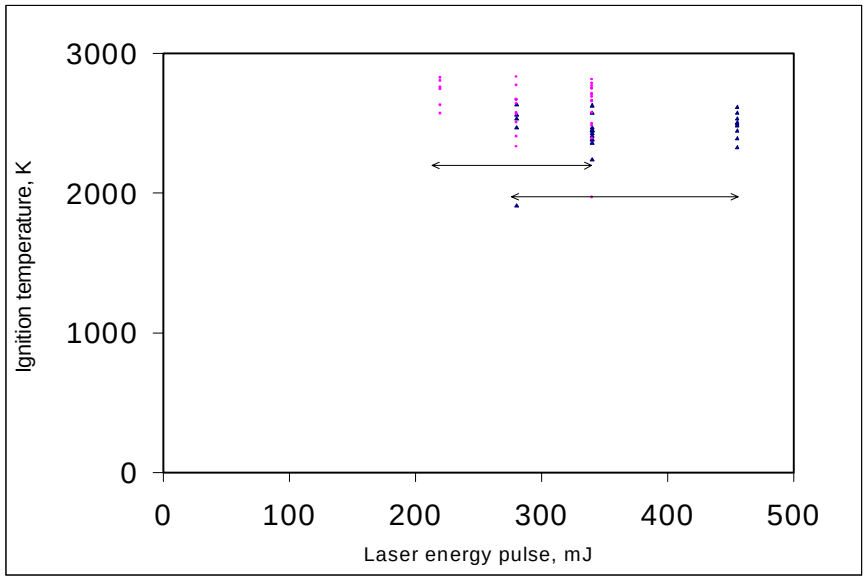

Figure 3.9. Distribution of ignition temperature versus laser energy for Pittsburgh #8 coal.

4. Computational Model

Recently, Chen (Chen, J.C. "Distributed Activation Energy Model of Heterogeneous Coal Ignition," *Combust. Flame*, 107, 291 (1996)) presented a new method for the analysis of heterogeneous ignition using the Distributed Activation Energy Model of Ignition (DAEMI). The model accounts for particle-to-particle variations in reactivity by describing a sample's reactivity with a single preexponential factor and a Gaussian distribution of activation energies among the particles.

The DAEMI models the conventional, drop-tube furnace ignition experiment by allowing for the particles within the coal sample to have a distribution of reactivity. It is prescribe that all the particles have the same properties, including the preexponential factor in the Arrhenius rate constant describing their ignition reactivity, and that their activation energy is distributed according to the Gaussian (or normal) distribution:

$$f(E) = \frac{1}{(2\pi\sigma^2)} \exp\left(\frac{-(E-E_0)^2}{2\sigma^2}\right) \tag{4.1}$$

where E_0 is the mean and σ is the standard deviation of the distribution. The expression

$$\int_E^{\Delta E} f(E)dE \tag{4.2}$$

describes the frequency or probability that particles within a sample have an activation energy in the range E to E +ΔE. Accordingly, the distribution satisfies the condition that $\int_{-\infty}^{\infty} f(E)dE = 1.$

The DAEMI divides a prescribed distribution into discrete energy intervals of $\Delta E = 1$ kJmol^{-1}, and considers only the energy range of E_0-3σ to E_0+3σ rather than -∞ to +∞. The latter simplification still covers 99.73% of the distribution. The model then calculates the frequency of being in each of these intervals by numerically integrating Eq. (4.2) for each of the intervals.

An ignition experiment is modeled by assuming that 10^5 particles are in the initial batch, and that they are distributed among the various ΔE intervals according to the calculated frequency for each interval. Each simulation of an experimental run under a given set of conditions is conducted on a batch of 100 randomly selected particles from the sample, keeping in mind that no particle can be selected more than once. Whether or not ignition occurs for a run is determined by the particle in the batch of 100 with the lowest activation energy. If this particle's reactivity equals or exceeds that determined by the critical ignition condition (that is, its activation energy is less than or equal to the critical energy determined from the ignition criteria), the batch is defined as ignited. This is consistent with the observation that single-particle ignition is discernible to the eye, and certainly to a photon detector. This procedure was repeated 20 times at each condition, just as in our actual experiments, to determine an ignition frequency at this condition. Finally, the laser pulse energy is varied several times and, each time, 20 simulations were conducted. The DAEMI exhibits the experimental characteristic of increasing ignition frequency with increasing gas temperature. This was expected since an increase in gas temperature leads to an increase in the maximum activation energies which a particle can have and still be ignitable, and therefore to an increased probability of having at least one particle which is reactive enough to ignite.

The DAEMI model captures the main characteristics of actual experiments: the gradual increase in ignition frequency with increasing gas temperature and the variation of the slope of the ignition frequency with O_2 concentration. Finally, it has been shown that adjustments to the model parameters can be used to fit experiment data and extract reaction rate constants. Although it was assumed that pulverized-coal ignition occurs heterogeneously without influence from any volatile matter that may be present, and even though the results closely fit the experimental data, DAEMI does not confirm that ignition is purely a heterogeneous process. Very few models of homogeneous ignition have been known, and none gave been tested against the available experimental data because of the inherent difficulty and uncertainty in modeling devolatilization and the combined solid-gas and gas-gas reactions.

Model Formulation

Figures 3.1 – 3.6 show typical data obtained from our ignition experiment conducted by varying the laser energy while fixing oxygen concentration, particle size and coal. Data from a conventional, drop-tube furnace experiment is compared to our data in Figures 4.1 and 4.2, and show that ignition frequency increases approximately linearly with laser pulse energy or gas temperature. These are inconsistent with the heterogeneous ignition theory previously described. If all particles of a coal sample used in an experiment have the same reactivity, that is if they are described by a common Arrhenius rate constant, then the data would show an ignition frequency of 0% until the critical laser energy corresponding to that at the critical ignition condition is reached. At any laser energy or gas temperature above critical ignition condition, the ignition frequency would be 100%.

One of the reasons why ignition frequency increases gradually with increasing laser energy or gas temperature is obvious: Within any coal sample, there exists a distribution of reactivity among the particles. Thus, in the laser ignition experiment, in which perhaps two particles from a batch 1300 particles of a sample heated by a laser pulse, there is an increasing probability (or frequency) that at least one particle has a reactivity that meets or exceeds the critical ignition condition set forth in the thermal ignition criteria as the laser energy is increased. This is the idea of DAEMI.

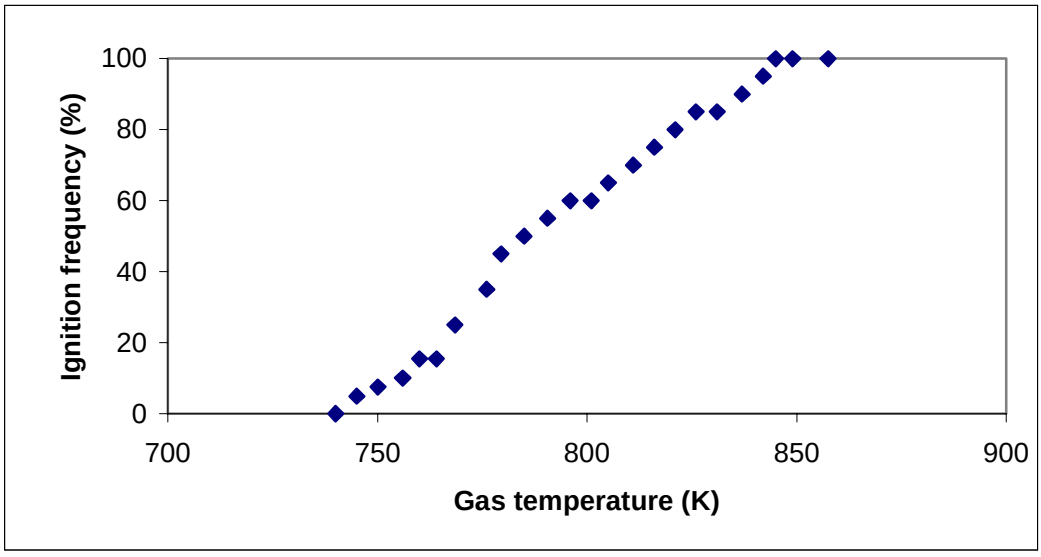

Figure 4.1. Typical data from a conventional ignition experiment showing the relation between ignition frequency and gas temperature for a bituminous coal.

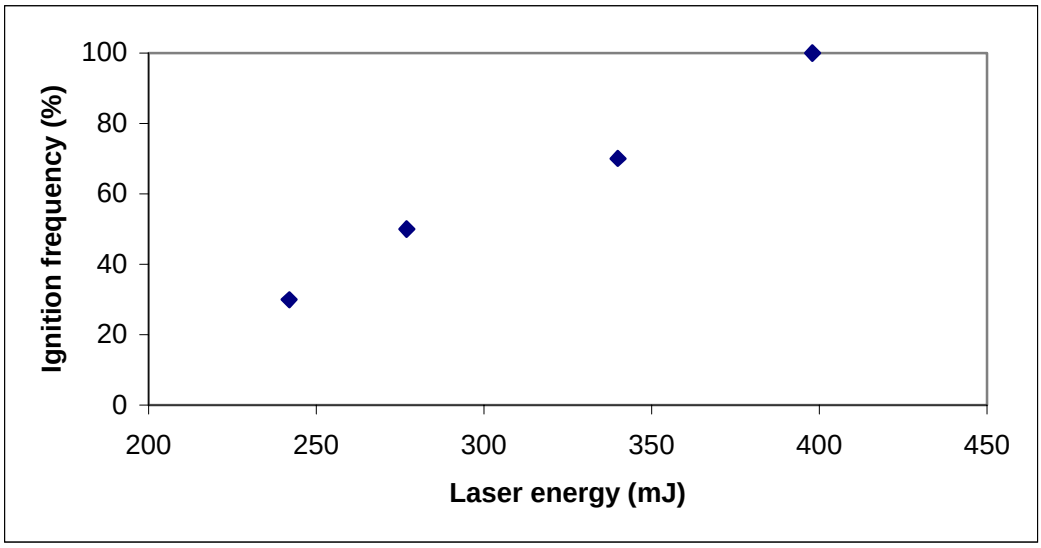

Figure 4.2. Typical data from our laser ignition experiment showing the relation between ignition frequency and laser energy for bituminous coal.

Of course, there exist other variations among the particles within a sample, such as particle size and specific heat. Variation in size alone could account for the observed increase in ignition frequency with the laser energy pulse (or gas temperature). It cannot account for other experimental observation, namely, the variation in the slope of the ignition frequency with oxygen concentration. A distribution in specific heat would only affect the rate at which a particle attains its equilibrium temperature, but would not change the value or the reactivity. Perhaps other variations could cause the observed behavior of ignition frequency. It is our premise that the distribution in reactivity and particle size dominates all other variations. We propose to add the distribution of particle size into the DAEMI.

Figure 4.3 shows the distribution of activation energy versus frequency for a sample for which E_0=58 kJ mol^{-1} and σ=5.5 kJ mol^{-1}. The intervals of activation energy is 1kJ mol^{-1} (ΔE=1kJ mol^{-1}).

The Distributed Activation Energy Model of Ignition (DAEMI) simulates the laser ignition and drop-tube experiments by allowing for the particles within the coal sample to have a distribution of reactivity. We first calculate the probability of particles for being in each of the intervals.

The distribution of particle sizes assumes that in a small range of particle size, the distribution of particle size has a top-hat distribution as shown in Figure 4.4. The interval of

particle size is 1μm ($\Delta Dp=1.0\times10^{-6}$m). Particle sizes are grouped into three groups: 106 to 125 μm, 125 to 150 μm, 150 to 180 μm.

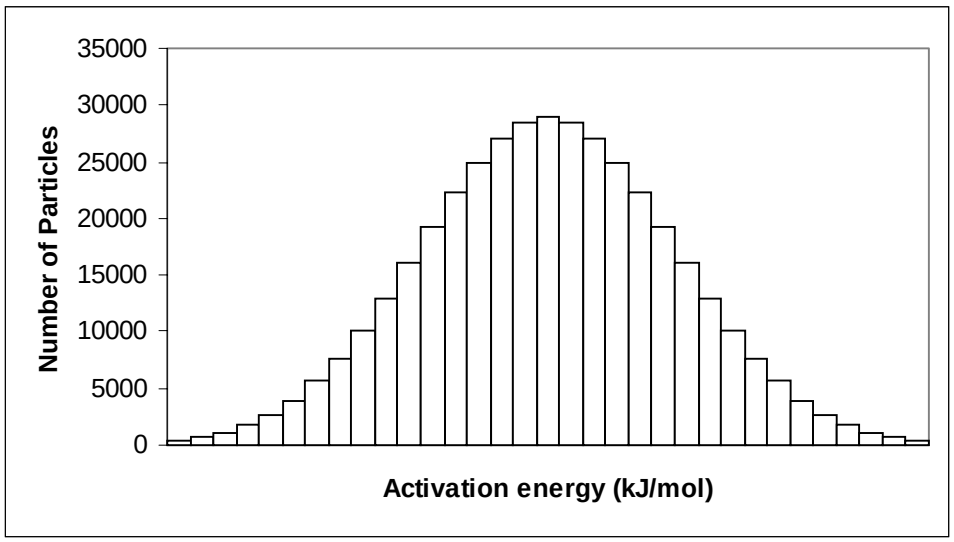

Figure 4.3. Distribution of activation energy as a Gaussian distribution.

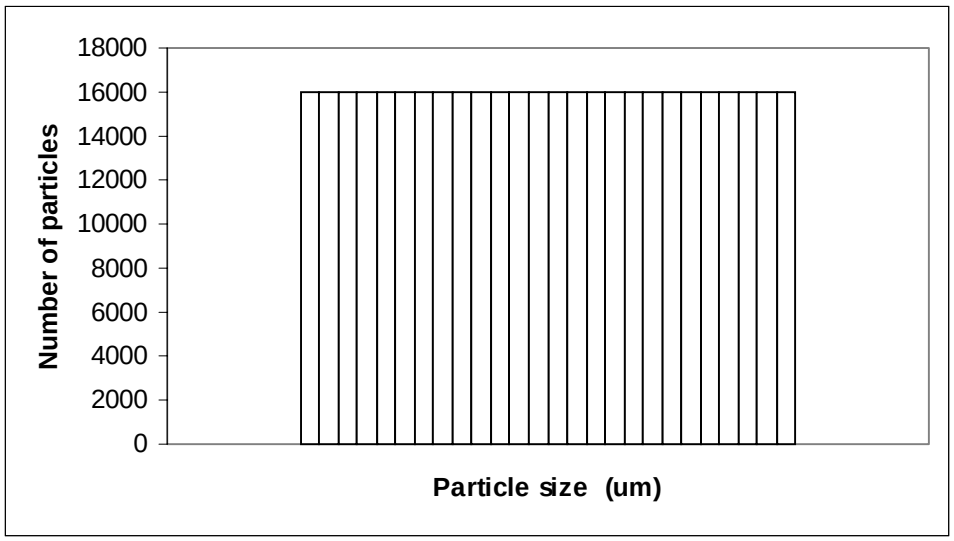

Figure 4.4. Distribution of coal particle size as a top-hat distribution.

Base Case

The heat generated by a spherical carbon particle undergoing oxidation on its external surface is given by the kinetic expression:

$$\frac{Q_{gen}}{S} = H_c x_{o_2}^n A_0 \exp\left(\frac{-E}{RT_p}\right) \tag{4.3}$$

Similarly, the heat loss from the surface of a particle at temperature T_p is the sum of losses due to convection and radiation. Thus, heat loss from the surface is given as:

$$\frac{Q_{loss}}{S} = hS(T_p - T_g) + \varepsilon\sigma_b S\left(T_p^4 - T_g^4\right) \tag{4.4}$$

For the convection-loss term, we assume that the Nusselt number equals 2, as is appropriate for very small particles, which leads to $h = 2k_g / d_p$.

$$\frac{Q_{loss}}{S} = \frac{2k_g}{d_p} S(T_p - T_g) + \varepsilon\sigma_b S\left(T_p^4 - T_g^4\right) \tag{4.5}$$

At the critical ignition condition, $Q_{gen} = Q_{loss}$, we obtain

$$E = -RT_p \ln\left(\frac{\left(\frac{2k_g}{d_p}\right)\left(T_p - T_g\right) + \varepsilon\sigma_b\left(T_p^4 - T_g^4\right)}{H_c x_{o_2}^n A_0}\right) \tag{4.6}$$

where the required parameters for this equation were calculated as follows.

For base case of the model, we assumed that T_p was obtained from the equilibrated temperature calculations by use of a linear regression to find Tp as a function of laser energy (see appendix 1). For example, for 70 μm, 116 μm and 165 μm coal particle the temperature are given as functions of laser energy as:

$$T_{p_{(116\,\mu m)}} = 0.7266E_{laser} + 385.22 \tag{4.7}$$

$$T_{p(70\,\mu m)} = 1.0707E_{laser} + 427.08 \tag{4.8}$$

$$T_{p(165\,\mu m)} = 0.5505E_{laser} + 367.57 \tag{4.9}$$

For variable particle size, we use the following interpolation scheme to calculate T_p:

$$T_p = \frac{\left(T_{p(70\,\mu m)} - T_{p(116\,\mu m)}\right)\left(d_p - 116e-6\right)}{(70-116)\times 1\times e-6} + T_{p(116\,\mu m)} \qquad d_p<116\mu m \tag{4.10}$$

$$T_p = \frac{\left(T_{p(165\,\mu m)} - T_{p(116\,\mu m)}\right)\left(d_p - 116e-6\right)}{(165-116)\times 1\times e-6} + T_{p(116\,\mu m)} \qquad d_p>116\mu m \tag{4,11}$$

The gas thermal conductivity in the boundary layer around a heated particle, k_g was given by a linear fit to the conductivity of air.

$$k_g = 7.0 \times 10^{-5} \left(\frac{T_p + T_g}{2} \right) \tag{4.12}$$

It is well known that the product of carbon oxidation is both CO and CO_2, $H'_{C,CO}$ and H'_{C,CO_2} are the heats of combustion corresponding to the following oxidation reaction.

$$\begin{aligned} C + \frac{1}{2} O_2 &\rightarrow CO; H'_{C,CO} = 9{,}210 \frac{kJ}{kgC} \\ C + O_2 &\rightarrow CO_2; H'_{C,CO_2} = 32{,}790 \frac{kJ}{kgC} \end{aligned} \tag{4.13}$$

H_c for ignition is defined by the equation [15]

$$H_c = \frac{y}{y+1} H'_{C,CO} + \frac{1}{y+1} H'_{C,CO_2} \tag{4.14}$$

Where

$$y = \frac{molCO}{molCO_2} = 59.95 \exp\left(\frac{-3214}{T_p} \right) \tag{4.15}$$

ε, the emissivity of coal particles was taken as 0.8.

n, the reaction order was taken as 1.

χ_{o2} was chosen to be 1.0 corresponding to a 100% oxygen concentration.

Figure 4.5 describes the simulation procedure for the base case laser experiment. First, the requisite parameters (A_0, n, E_0 and σ) are assumed, then the range of laser energy is selected so as to obtain an ignition frequency from 0% to 100%. The particle temperatures are estimated by equation (4.7)-(4.11). A batch of 1300 particles is randomly selected from the total particles with the distribution of activation energy and particle size. M particles that are assumed to be heated by pulse laser randomly selected from 1300 particles. For each of M particles, the particle size (d_p) and activation energy (E_{min}) are randomly assigned. The activation energy (E_{max}) is calculated by equation (4.6).

For each particle, E_{max} is compared with the expected activation energy (E_{min}) of a particle. If $E_{max} \geq E_{min}$, the particle is considered "ignited". If $E_{max} < E_{min}$, the particle is not ignited. For each laser energy, a new batch was selected and the process repeat 20 times. The 20 runs are made and the ignition-frequency is obtained at that laser energy. The laser energy is then changed and the process repeated.

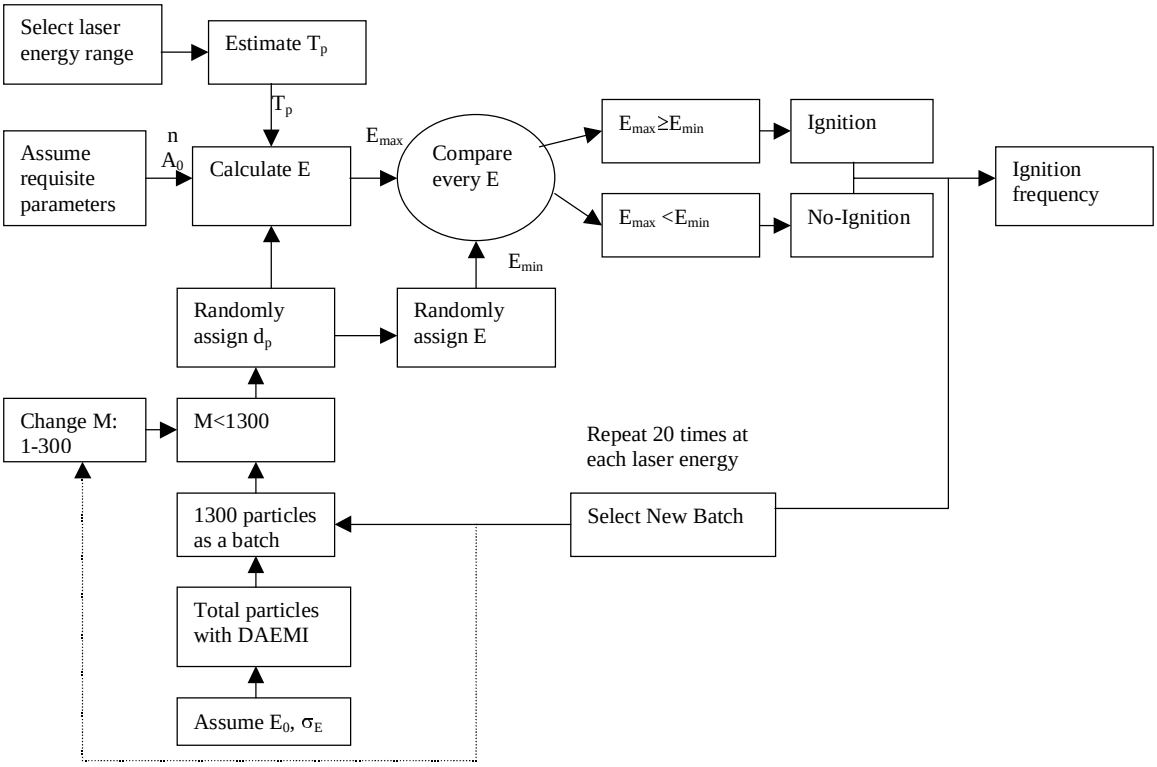

Figure 4.5. Simulation procedure for base case of the laser experiment

For different experiment mechanism, the particles heated for a batch are different. So we analyzed the effect of M on the ignition frequency by changing the values of M from 1 to 300.

To analyze the effect of the particle size distribution, we use both of distribution and average particle size into DAEMI. This is done by using average particle size when specifying or randomly selected d_p from the range d_{min} to d_{max}.

laser Ignition Experiment

To model the ignition experiment, measured temperatures were used in the DAEMI in order to fit the experiment data. The experiment data of Tp was read directly from data files (see appendix 3), and used to calculate average temperature (T_{avg}) and standard deviation (T_σ), base on Normal distribution,

$$T_{avg} = \frac{\sum T_p}{N} \qquad \text{(N is the number of } T_p\text{)} \qquad (4.16)$$

$$T_{\sigma} = \sqrt{\frac{\sum (T_p - T_{avg})^2}{N-1}} \qquad (4.17)$$

to obtain the range of temperature, namely, $T_{avg}-2T_{\sigma} < T_p < T_{avg}+2T_{\sigma}$, by randomly choosing particle temperature from the range to obtain critical energy at each condition.

In this experiment, a batch with several hundred particles is dropped in to the test section and only the laser pulse heats a few particles. There is an increasing probability (or frequency) as the laser energy is increased that at least one of the heated particles is reactive enough to ignite under the given conditions. For nearly every case, one to three particles are hit in the test section by the two intersecting laser beams. This is determined by observations with high-speed video. For simulation, thirteen hundred particles are selected randomly as the feed into the test section and two particles are further selected randomly from these 1300 to be hit by the laser pulse.

Figure 4.6 describes the simulation procedure for the laser experiment. We consider 1300 particles as a batch size randomly selected from the total number of particles. Using the distribution of activation energy and particle size, two particles randomly selected from 1300 particles are assumed heated by pulse laser. For each particle randomly selected from two (M) particles, particle size (d_p) and activation energy (E_{max}) are randomly assigned. Pre-exponential factor (A_0), mean of Gaussian distribution of activation energy (E_0), standard deviation of Gaussian distribution (σ) and reaction order (n) in Eq. (3.4) are assumed. E_{max} is calculated as the critical (or threshold) activation energy under the given conditions. The result (E_{max}) is compared with the activation energy (E_{min}) of a particle. If the result (E_{max}) is greater than the activation energy (E_{min}), then the particle is considered ignited and the run is successful.

At each laser energy, a new batch is selected and the process repeated 20 times, the 20 runs are used to obtain the ignition-frequency at that energy level. At each set of operating conditions (coal type, particle size and oxygen concentration), the modeling results are compared with the experimental results over the range of laser energy. If the modeling results do not fit the experiment results, we modify these parameters (E_0, σ, A_0 and n) and repeat the process.

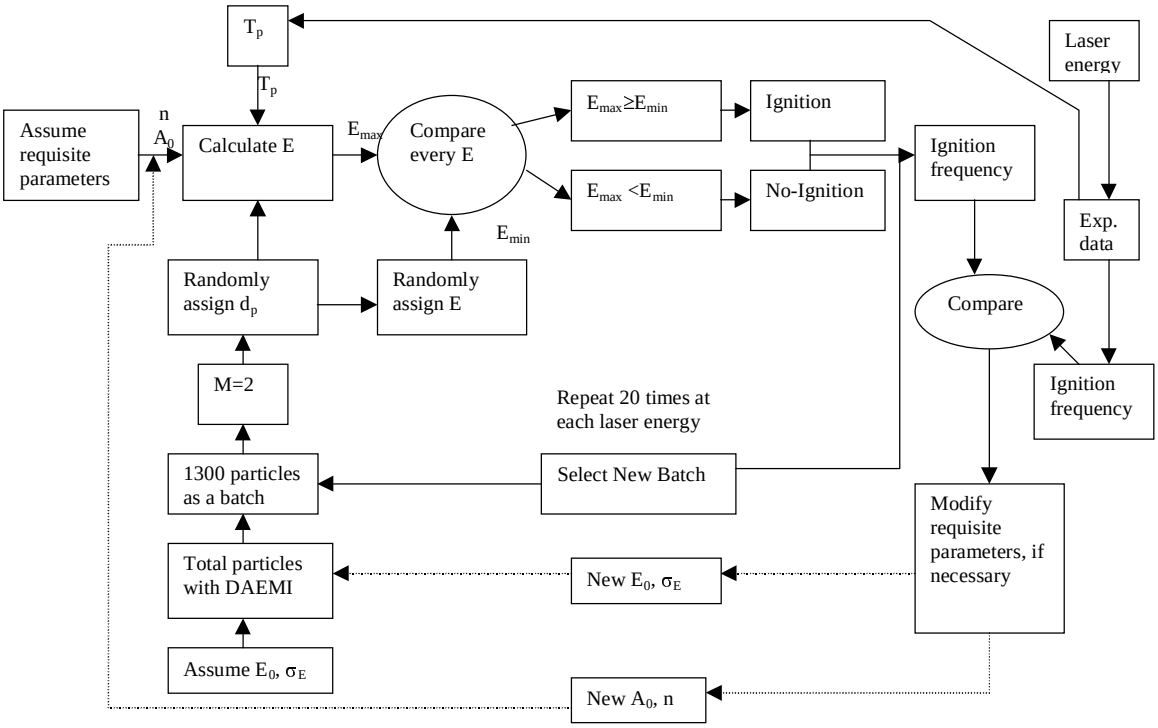

Figure 4.6. Simulation procedure for the laser experiment.

Drop-Tube Experiment

In simulating the drop-tube ignition experiment, we assumed that 10^6 particle are in the initial batch. A batch of 1170 particles of a sample is dropped into the furnace in each simulation of an experimental run. No particle can be selected more than once. Now, using Eq. (3.1) and Eq. (3.3) we can obtain the heat generated Q_{gen} and Q_{loss}.

In order to determine the critical ignition temperature of the particle, Tp, and critical activation energy, E, the critical ignition condition, $Q_{gen} = Q_{loss}$, and $\frac{dQ_{gen}}{dT_p} = \frac{dQ_{loss}}{dT_p}$ are solved simultaneously. Q_{gen} and Q_{loss} are given in Eqs. (3.1) and (3.3), and lead to the following derivatives with respect to temperature:

$$\frac{dQ_{gen}}{dT_p} = SH_c x_{o_2}^n A_0 \exp\left[\frac{-E}{RT_p}\right]\left(\frac{E}{RT_p^2}\right) \tag{4.18}$$

$$\frac{dQ_{loss}}{dT_p} = \frac{2k_g}{d_p} S + 4\varepsilon\sigma_b S T_p^3 \tag{4.19}$$

Note that the neglection of the T_p dependence in k_g introduces a small error in Eq. (4.19).

Following $\frac{dQ_{gen}}{dT_p} = \frac{dQ_{loss}}{dT_p}$, we set Eq. (4.18) equal to Eq. (4.19) and solve for the quantity E/RT_p:

$$\frac{E}{RT_p} = \frac{\frac{2k_g}{d_p}T_p + 4\varepsilon\sigma_b T_p^4}{H_c x_{o_2}^n A_0 \exp\left[\frac{-E}{RT_p}\right]} \tag{4.20}$$

The denominator is recognized to be Q_{gen}/S in Eq. (3.1), which by $Q_{gen} = Q_{loss}$ is also Q_{loss}/S in Eq. (4.3). Thus Eq. (4.20) can be rewritten as:

$$\frac{E}{RT_p} = \frac{\frac{2k_g}{d_p}T_p + 4\varepsilon\sigma_b T_p^4}{\frac{2k_g}{d_p}(T_p - T_g) + \varepsilon\sigma_b(T_p^4 - T_g^4)} \tag{4.21}$$

This relation for E/RT_p is substituted into the expression $Q_{gen} - Q_{loss} = 0$ to obtain a function, F, which is a function of T_p only:

$$\begin{aligned} F(T_p) &= Q_{gen} - Q_{loss} \\ &= H_c x_{o_2}^n A_0 \exp\left[\frac{\frac{2k_g}{d_p}T_p - 4\varepsilon\sigma_b T_p^4}{\frac{2k_g}{d_p}(T_p - T_g) + \varepsilon\sigma_b(T_p^4 - T_g^4)}\right] - \frac{2k_g}{d_p}(T_p - T_g) - \varepsilon\sigma_b(T_p^4 - T_g^4) = 0 \end{aligned} \tag{4.22}$$

The reasonable root of $F(T_p)$ corresponds to the critical ignition temperature of the particle, and substitution of this value into equation (4.21) produces the critical activation energy at the critical ignition condition.

k_g, the gas thermal conductivity in the boundary layer around a heated particle was given by equation (4.12). χ_{o2} was chosen to be 0.5 corresponding to a 50% oxygen concentration. ε, the emissivity of coal particle was taken as 0.8. H_c was defined by the equation from (4.13) to (4.15).

Figure 4.7 describes the simulation procedure for the drop-tube experiment. First, the requisite parameters (A_0, n, E_0 and σ) are assumed. We consider 1170 particles as a batch size randomly selected from the total number of particles using the distribution of activation energy

and particle size. M particles randomly selected are considered heated by the hot gas. For each of the M particles, the particle size (d_p) and activation energy (E_{min}) are randomly assigned. Substituting all the required values in equation (4.22) permits the calculation of the particle temperatures from the gas temperatures. Substituting all the required values in equation (3.19) the critical (or threshold) activation energy (E_{max}) is calculated for the given ignition conditions. For each particle, E_{max} is compared with the activation energy (E_{min}). If $E_{max} \geq E_{min}$, the particle is said to be ignited, and the run also is considered successful. If $E_{max} < E_{min}$, the particle is not ignited.

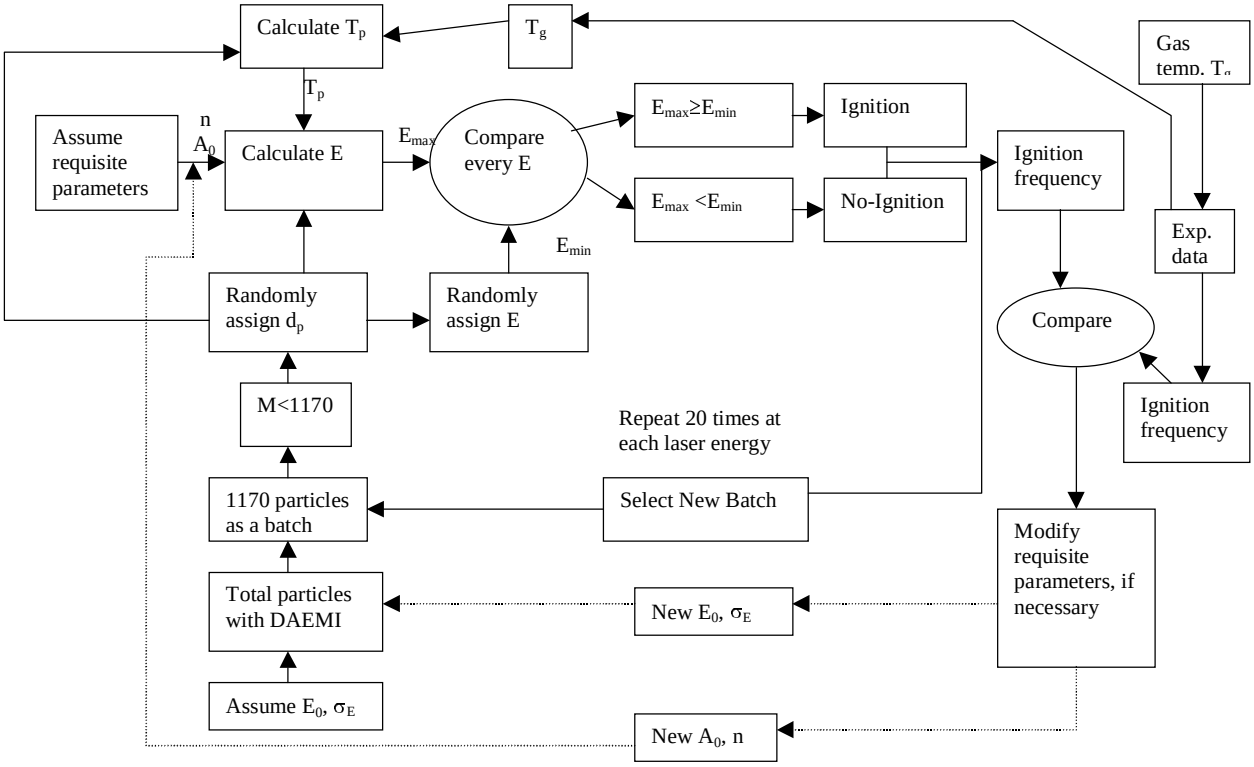

Figure 4.7. Simulation procedure for the drop-tube experiment.

For each gas temperature, a new batch is selected and the process repeated 20 times, the 20 runs enable the ignition-frequency to be obtained. At each set of operating conditions (coal type, particle size and oxygen concentration), the modeling results are compared with the experimental results over the range of gas temperatures. If the modeling results do not fit the experiment results, we modify these parameters (E_0, σ, A_0. and n) and repeat the process.

Other simulation methods used the average particle size and randomly assigned a particle in the batch of 1170 with the lowest activation energy (E_{min}). The result (E_{max}) is compared

with the lowest activation energy (E_{min}). If the E_{max} is greater than the lowest activation energy E_{min} among the particles that is heated in a run, then the particle is ignited

5. Modeling Results

Results of the Base Case of the Model

Figure 5.1 and Figure 5.2 show the effect of oxygen concentration and number of particles (M) on ignition frequency for particle size range of 106-125μm and 150-180μm, respectively. It can be seen that at each oxygen concentration, ignition frequency increases monotonically over the range of laser pulse energy. Below this range, the ignition frequency is zero, and above this range the result is 100% ignition frequency. As the number of particle (M) that is selected from the batch of 1300 particles is increased from 1 to 300, the frequency distribution shifts to lower laser energy values. This behavior is due to the fact that, within any coal sample, a distribution of reactivity exists among the particles.

As the oxygen concentration is decreased from 100% to 67%, the frequency distribution shifts to higher laser energies or equivalently, higher particle temperatures, as expected. This is consistent with the ignition theory since at decreased oxygen concentration, higher temperatures are necessary for heat generation by the particles (due to chemical reactions) to exceed heat loss from the particles and lead to ignition. The shift in distribution can be viewed in two ways: for a fixed laser pulse energy, a decrease in oxygen concentration leads to a decrease in the ignition frequency, all else being equal. Second, a decrease in oxygen concentration implies that the higher laser pulse energy is needed, in order to achieve the same ignition frequency.

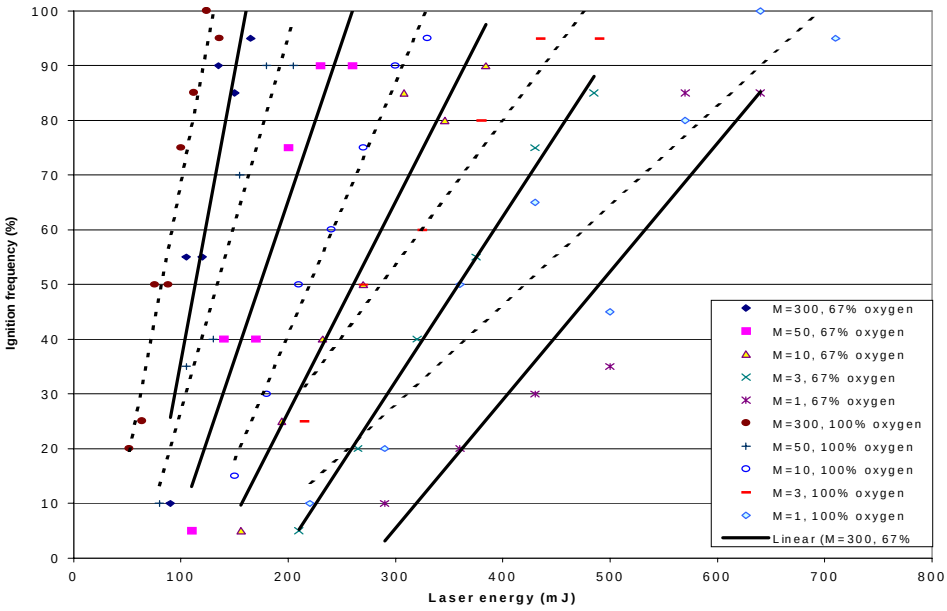

Figure 5.1. Modeling results showing the effect of M and oxygen concentration on ignition frequency. (a) Solid-line express 67% oxygen concentration (x_{o2} =67%); (b) Dash-line express 100% oxygen concentration (x_{o2} =100%). Particle size is 106-125 μm.

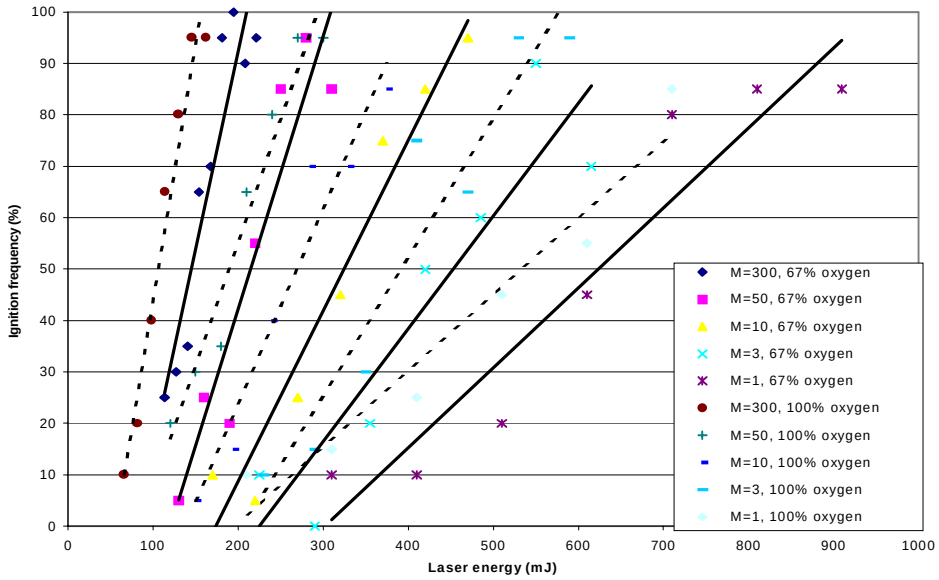

Figure 5.2 Modeling results showing the effect of M on ignition frequency. (a) Solid-line express 67% oxygen concentration (x_{o2} =67%); (b) Dash-line express 100% oxygen concentration (x_{o2} =100%). Particle size is 150-180 μm

Figure 5.3 and Figure 5.4 show the effect of particle size distribution in 150-180μm and average particle size 165μm on ignition frequency for oxygen concentrations of 100% and 67%.

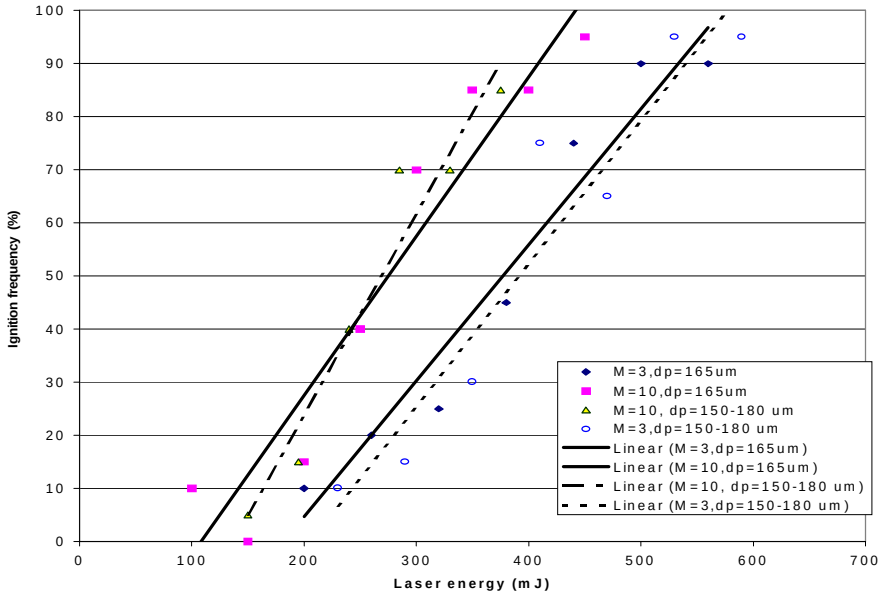

Figure 5.3 Modeling results showing the effect of average particle size 165μm and the range of particle size 150-180μm in ignition frequency. Oxygen concentration is 100%. (a) Solid-line express particle size d_p=165μm; (b) Dash-line express distribution particle size D_p in 150-180μm.

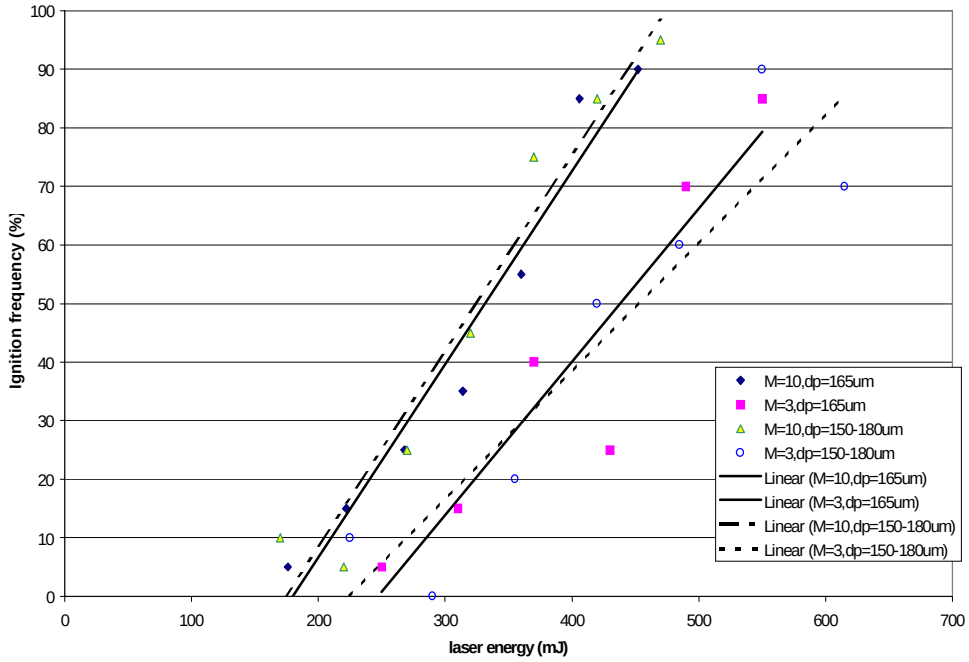

Figure 5.4 Modeling results showing the effect of the average particle size 165μm and the range of particle size150-180 μm on ignition frequency. Oxygen concentration is 67%. (a) Solid-line express particle size d_p=165μm; (b) Dash-line express distribution particle size d_p in 150-180μm.

Results of Simulation of Laser Ignition Experiment

The simulations for the experiments were performed via a FORTRAN code. The code was designed to produce frequency distribution data for a given particle size range, oxygen concentration, temperature of particle, and laser pulse energy. As discussed earlier, for each run two particles are selected randomly from 1300 particles. The particle size and activation energy are determined whether or not ignition occurred for the run. For each type coal, the parameters required as input are the average activation energy (E_0), standard deviation for the Gaussian distribution (σ), and pre-exponential factor (A_0).

Figures 5.5 – 5.7 show the experiment data for the Pittsburgh #8 coal with modeling results, which calculate average temperature and standard deviation to obtain the range of particle temperature at each condition. The behavior of the model with respect to changes in each of the parameters was first observed. The parameters are then modified to obtain a final set of values to improve the model. The final parameters that fit our laser ignition experimental data for the Pittsburgh #8 coal are given Table 3.1. Simulations for other coal types is similar to those shown in these figures

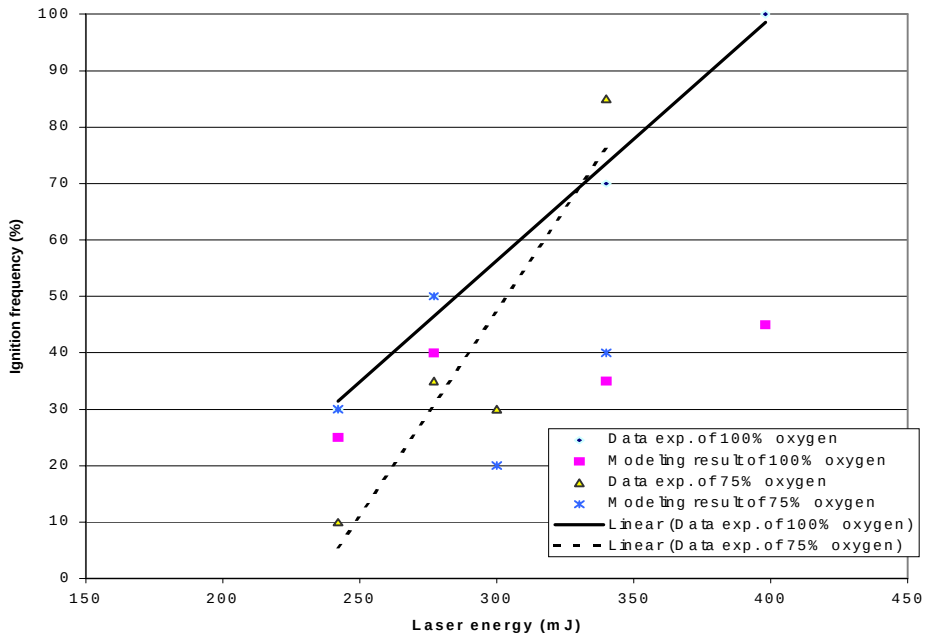

Figure 5.5 Simulation results of our laser experiment for particle size (d_p) 106-125μm Pittiburgh#8 coal, using the range of the particle temperatures.

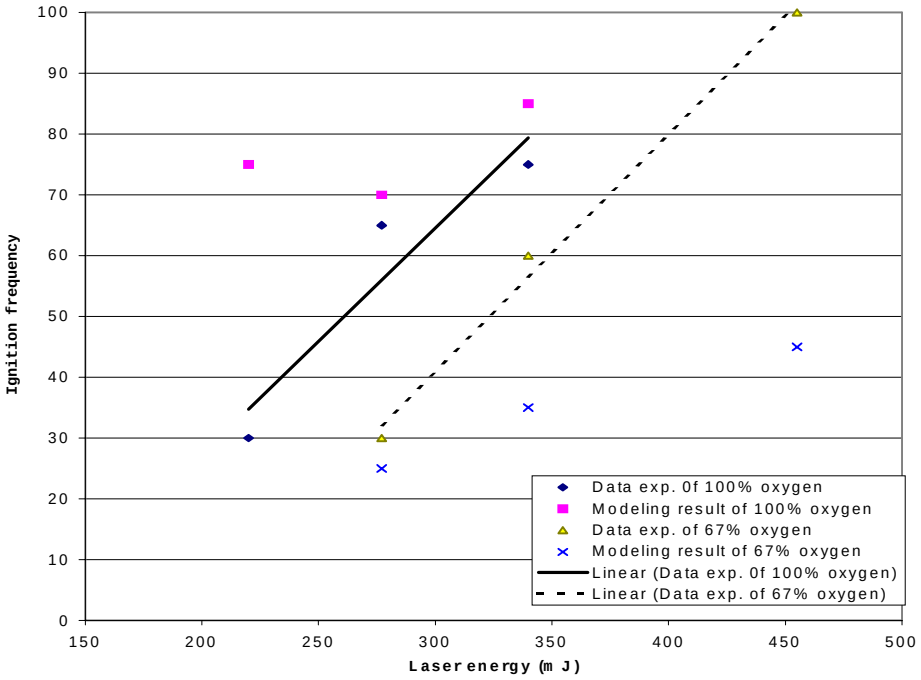

Figure 5.6 Simulation results of our laser experiment for particle size (d_p) 150-180μm Pittiburgh#8 coal, using the range of the particle temperatures.

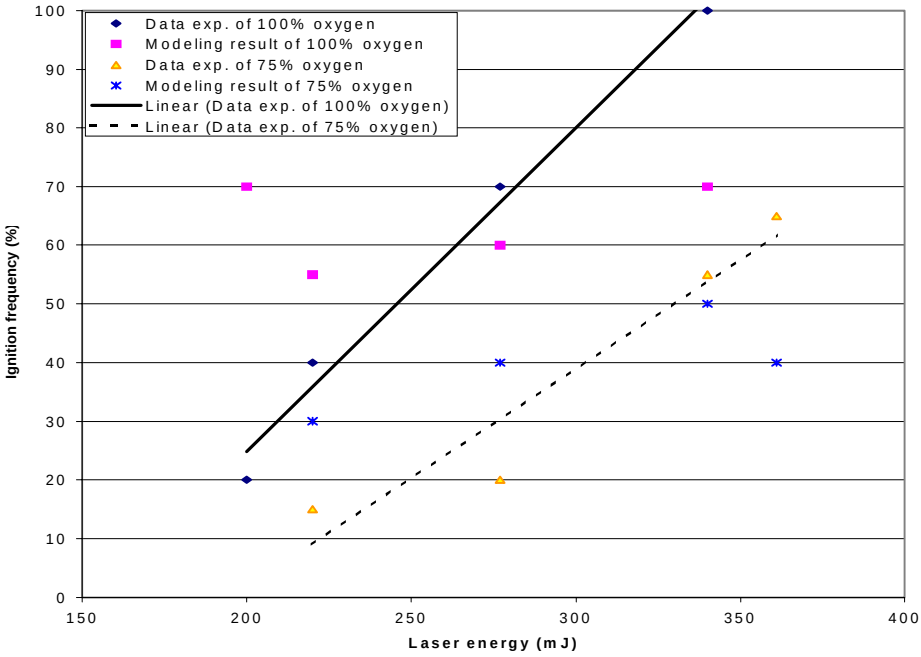

Figure 5.7 Simulation results of our laser experiment for particle size (d_p) 125-150μm Pittiburgh#8 coal, using the range of the particle temperatures.

Table 3.1. Simulation parameters for Pittsburgh#8 coal in laser ignition experiment.

Variable	Value
E_0	135 kJ/mol
A_0	250 kg/m^{2}s
σ	12 KJ/mol
n	1
ε	0.8

Results of The Drop-Tube Experiment

The required simulations for drop-tube experiments have been performed by a FORTRAN code. The code was designed to produce frequency distribution data for a given average particle size (diameter d_p) and the maximum diameter (dp, max) and minimum diameter (dp, min) of particle size range, oxygen concentration and, gas temperature. Figures 5.8 – 5.11 show the same effect of particle size distribution in 75-90 μm and average particle size 83 μm on ignition frequency for oxygen concentration from 10% to 100%. Respectively, Figures 5.8 – 5.9 show the experiment data for coal#1 and coal#2 with the modeling results using distribution of particle size. Figure 5.10 – 5.11 show the experiment data for coal#1 and coal#2 with the modeling results by average particle size. There are all parameters of coal#1 and coal#2 in Table 5.2 and Table 5.3.

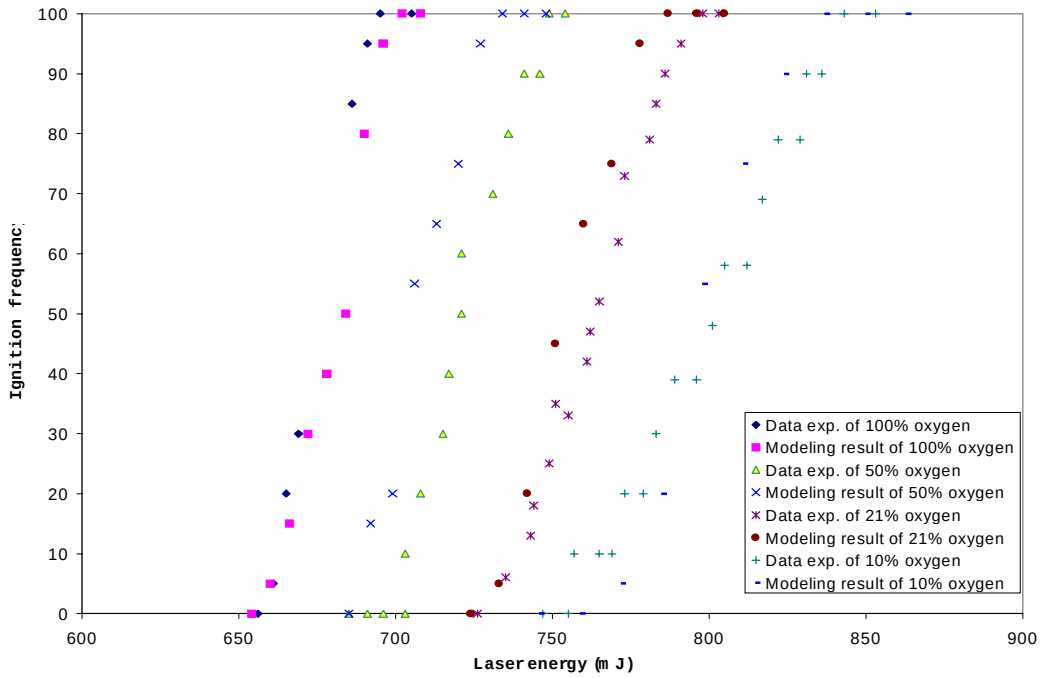

Figure 5.8. Simulate result of drop-tube experiment for the range particle size 75-90μm coal #1, using distribution particle size is incorporated into the DAEMI.

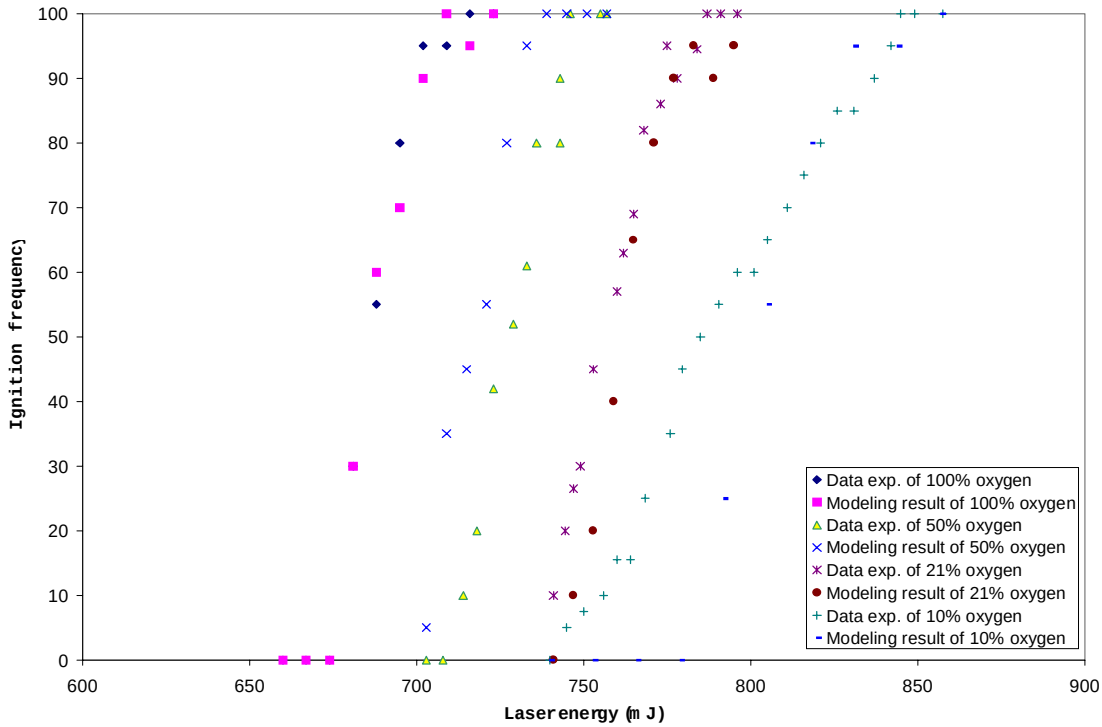

Figure 5.9. Simulation results of drop-tube experiment for the range particle size 75-90 μm coal#2, using distribution particle size is incorporated into the DAEMI.

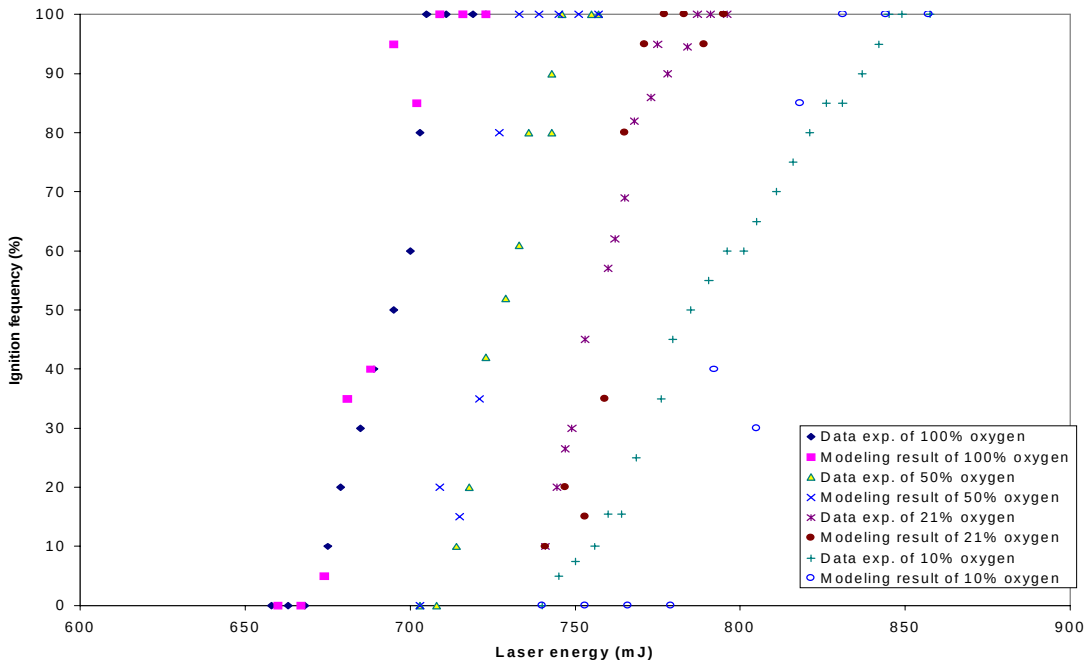

Figure 5.10. Simulate result of drop-tube experiment for particle size 83 μm coal #2, using average particle size into the current version of DAEMI.

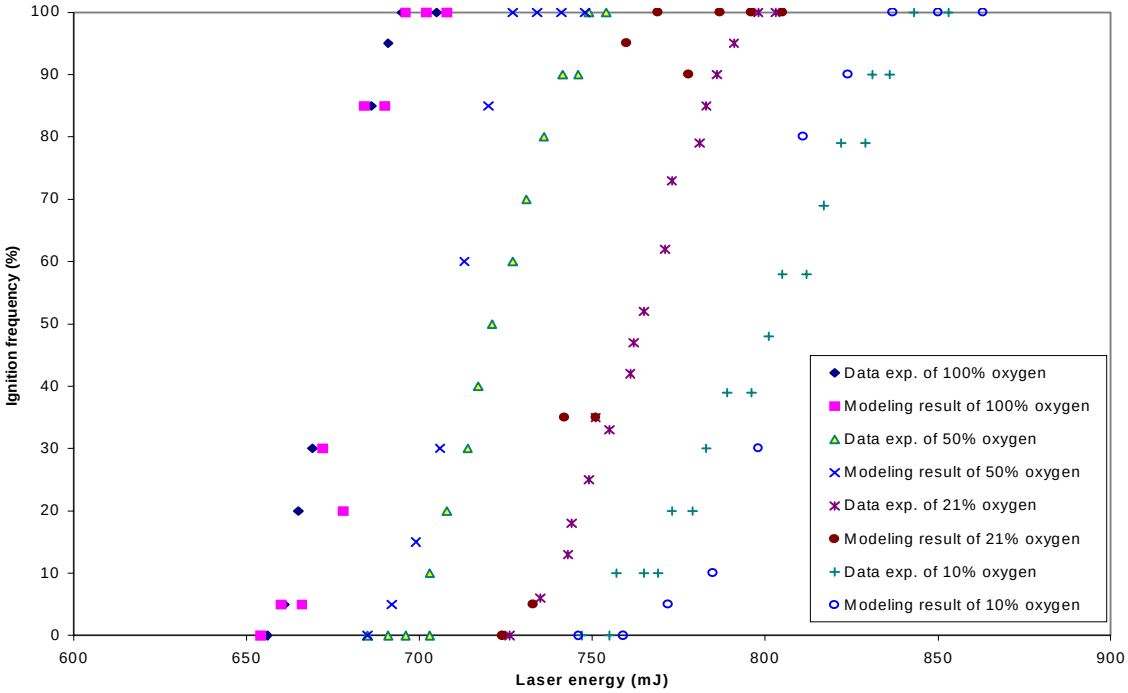

Figure 5.11. Simulate result of drop-tube experiment for particle size 83 μm coal #1, using average particle size into the current version of DAEMI.

Table 5.2. Simulation parameters for cola#1 in drop-tube experiment, using distribution and the average of particle size in current version DAEMI.

Variable	Value
E_0	70.0 (kJ/mol)
A_0	300.0 (kg/m^{2}s)
σ	1.0 (KJ/mol)
n	0.5
ε	0.8

Table 5.3. Simulation parameters for cola#2 in drop-tube experiment, using distribution and the average of particle size in current version DAEMI.

Variable	Value
E_0	71.0 (kJ/mol)
A_0	320.0 (kg/m^{2}s)
σ	1.0 (KJ/mol)
n	0.5
ε	0.8

CONCLUSIONS

In this project, we investigated fundamental aspects of coal ignition through (1) experiments to determine the ignition temperature of various coals by direct measurement, and (2) modeling of the ignition process to derive rate constants and to provide a more insightful interpretation of data from ignition experiments.

The specific objectives of this project were:

1. develop a novel experimental facility with extensive optical-diagnostic capabilities to study coal ignition;
2. determine the ignition temperature of coals under simulated combustion conditions by direct measurement with two-color pyrometry;

3. examine the effects of various experimental conditions, including coal rank, particle size, oxygen concentration and heating rate, on the ignition temperature;
4. determine the ignition rate constants of various coals.
5. modify our existing ignition model to examine the effect of particle-size distribution on the ignition behavior;
6. incorporate, if necessary, a size distribution into the model;
7. apply the model to extract ignition rate constants from previously published data from conventional experiments;
8. modify the model and apply it to our laser-based ignition studies for determination of ignition rate constants.

All of the project objectives were achieved in the period of this grant. Some specific findings from this project are:

1. ignition temperatures measured using our laser-ignition experiment showed a wide range of values, due most likely to the wide distribution of reactivity among coal particles within a sample;
2. there is no apparent relation between coal rank and reactivity distribution, as determined by our model of ignition (DAEMI);
3. ignition temperatures were highest for the Pittsburgh #8, high-volatile bituminous coal and was lower for both the Pust lignite and Wyodak subbituminous coal, both of which showed similar ignition temperatures;
4. based on #3 above, it is concluded that the ignition reactivity is highest for the high-volatile bituminous coal, and is lower for the lignite and subbituminous coals, consistent with the combustion reactivity of these coal types;
5. the DAEMI base case showed that the results are sensitive to the number of particles (M) considered in the model, as expected;
6. the DAEMI base case showed that the model is insensitive to the particle size distribution, as a top-hat distribution gave similar results to that found using a constant particle size;
7. the DAEMI, although capable of capturing the behavior of the laser-ignition experiment, could not be adjusted to accurately model the results, due most likely to the wide range of ignition temperatures measured;

8. the DAEMI accurately modeled the results from a conventional drop-tube furnace experiment based on two coals and a wide range of particle sizes and oxygen concentration, and was successful in extracting the ignition rate constants.

BIBLIOGRAPHY

Experiment

1. Essenhigh, R. H., Mahendra, K. M., and Shaw, D. W. Ignition of coal particles: A Review. Combustion and Flame 77:3-30, 1989.
2. Cassel, H.M. and I. Liebman. The Cooperative Mechanism in the ignition of Dust Dispersions. Combustion and Flame 3:467-475, 1959.
3. Chen, J.C., Masayuki Taniguchi, Kiyoshi Narato and Kazuyuki Ito. Laser Ignition of Pulverized Coals. Combustion and Flame 97:107-117, 1994.
4. Bandyopadhyay, S., and Bhaduri, D. Prediction of Ignition Temperature of a Single Coal Particle. Combustion and Flame 18:411-415, 1972.
5. Wall, T. F. and Gururajan, V. S. Combustion Kinetics and the Heterogeneous Ignition of Pulverized Coal. Combustion and Flame 66:151-157, 1986.
6. Gupta, R. P., Gururajan, V. S., Wall, T. F., and Lucas, J. A. Ignition Temperature of Pulverized Coal Particle: Experimental technique and Coal-Related Influences Combustion and Flame 79:333 – 339, 1990.
7. Wall, T. F., Gupta, R. P., Gururajan, V. S., and Zhang, D. The Ignition, Burning rate and Reactivity of Petroleum Coke. Twenty-third Symposium (International) on Combustion/ The Combustion Institute, Pittsburgh, 1990, (1177-1183).
8. Tognotti, L., Malotti, A., Petarca, L., and Zonelli, S. Measurement of Ignition Temperatures of Coal Particles Using a Thermogravimetric Technique. Combust. Sci. and Tech., 1985, Vol. 44, (15-28).
9. Boukara, R., Gadiou, R., Gilot, P., Delfosse, L., and Prado, G. Study of the Ignition of single coal and char particles in a drop-tube furnace by a probability method. Twenty-fourth Symposium (International) on Combustion /Combustion Institute, Pittsburgh, 1993, (1127-1133).
10. Tomeczek, J. and Wojcil, J. A Method of Direct Measurement of Solid Fuel Particle Ignition Temperature. Twenty-third Symposium (International) on Combustion / The Combustion Institute, Pittsburgh, 1990, (1163-1169).
11. Karcz, H., Korod, W., and Rybak, W. Evaluation of Kinetic Parameters of Coal Ignition. Fuel, 1980, Vol. 59, November (799-802).
12. Wall, T. F., Gupta, R. P., Gururajan, V. S., and Dong-Ke Zhang. The Ignition of coal particles. Fuel, 1991, Vol. 70, September (1011-1016).
13. Zhang, D., Wall, T. F., Harris, D. J., Smith, w., Chen, J., and Stanmore, B. R. Experimental studies of Ignition behavior and combustion reactivity of pulverized fuel particles. Fuel, 1992, Vol. 71 November, (1239-1246).

14. Dong Ke Zhang, Wall, T. F., and Tate, A. G. The Reactivity of Pulverized Coal Char Particles: experiments using ignition, burnout, and DTG techniques and partly burnt chars. Fuel 71:1247-1253, 1992.

15. Dong Ke Zhang, and Wall, T. F. Ignition of coal particles: the influence of experimental technique. Fuel, 1994 Vol. 73 (1114-1119).

16. Phouc, T. X., Mathur, M. P., and Ekman, J. M. High-Energy Nd-Yag Laser Ignition of Coals: Experimental Observations. Combustion and Flame, 93:19-30, 1992.

17. Zhang, D. Laser Induced Ignition of Pulverized Particles. Combustion and Flame, 90:134-142, 1992

18. Hills, P. C., Zhang, P. J., and Wall, T. F. Laser-Ignition of Combustible Gases by Radiative Heating of Small Particles. Combustion and Flame, 91:399-412, 1992.

19. Wong, B. A., Gavalas, G. R., and Flagan, R. C. Laser Ignition of Levitated Char Particles. Fuel 1995 Vol. 9 (484 – 492)

20. Cozzani V., Pertaca L., Tognotti, L., and Pintus S. Ignition and Combustion of single Levitated Char Particles. Combustion and Flame, 103:181-193, 1995.

21. Qu, M., Ishigaki, M., and Tokuda M. Ignition and Combustion of Laser-Heated Pulverized Coal. Fuel 1996 Vol. 75 (1155 – 1160)

22. Musti, S. S. Ignitability of Various Coals as Measured by Laser Ignition. Masters Degree of Chemical Engineering, Department of North Carolina A & T State University, 1996.

Computational Model

23. Cassel, H.M. and I. Liebman. The Cooperative Mechanism in the Ignition of Dust Dispersions. Combustion and Flame 3:467-475, 1959.

24. Wall, T.F., R. P. Gupta, V. S. Gururajan and Dong-ke Zhang. The ignition of coal particles. Fuel, 1991,Vol 70, September (1011-1016).

25. Chen, J.C., Masayuki Taniguchi, Kiyoshi Narato and Kazuyuki Ito. Laser Ignition of Pulverized Coals. Combustion and Flame 97:107-117, 1994.

26. Zheng, D., Wall, T. F., Harris, D. J., Smith, I. W., Chen, J., and Stanmore, B. R.. Experimental studies of ignition behavior and combustion reactivity of pulverized fuel particles. Fuel, 1992, Vol 71November, (1239-1246).

27. Boukara, R., Gadiou, R., Gilot, P., Delfosse, L., and Prado, G. Study of The ignition of single coal and char particles in a drop tube furnace by a probability method. Twenty-Fourth Symposium (Intermational) on Combustion / Combustion Institute, Pittsburgh, 1993, (1127-1133).

28. Chen, J.C.. Distributed Activation Energy Model of Heterogeneous Coal Ignition. Combust. Flame 107:291-298, 1996.

29. Dong Ke Zhang, T. F. Wall. Ignition of coal particles: the influence of experimental technique. Fuel, 1994, Volume 73 Number 7 (1114-1119).

30. Essenhigh, R. H., Mahendra, K.M., and Shaw, D.W. Ignition of coal particles: A Review. Combustion and Flame 77:3-30, 1989.

31. Bandyopadhyay, S., and Bhaduri, D. Prediction of Ignition Temperature of a Single Coal Particle. Combustion and Flame 18:411-415, 1972.

32. Karcz, H., W. Korod and W. Rybak. Evaluation of Kinetic Parameters of Coal Ignition. Fuel, 1980, Vol 59, November (799-802).

33. Wall, T.F., V. S. Gururajan. Combustion Kinetics and the Heterogeneous Ignition of Pulverized coal. Combustion and Flame 66: 151-157, 1986

34. Dong-ke Zhang, Terry F. Wall and Anthony G. Tate. The reactivity of pulverized coal char particles: experiments using ignition, burnout and DTG techniques and partly burnt chars. Fuel 71:1247-1253, 1992.

35. Zhang, D. Laser-Induced Ignition of Pulverized Fuel Particles. Combustion and Flame, 90:134-142, 1992.

36. Phuoc, T. X., Mathur, M, P., and Ekmann, J. M. High-Energy Nd-Yag Laser Ignition of Coals: Experimental Observations. Combustion and Flame, 93:19-30, 1993.

37. Hills, P.C., D. K. Zhang, P. J. Samson, and T. F. Wall. Laser Ignition of Combustible Gases by Radiative Heating of Small Particles. Combustion and Flame, 91:399-412, 1992.

38. Tomeczek, J., and Wojcil, J. A method of direct measurement of solid fuel particle ignition temperature. Twenty-Third Symposium (International) on Combustion/The Combustion Institute, Pittsburgh, 1990, (1163-1169).

39. Leonardo Tognotti, Andrea Malotti, Luigi Petarca, and Severino Zonelli. Measurement of Ignition Temperature of Coal Particles Using a Thermogravimetric Technique. Combust. Sci. and Tech., 1985, Vol. 44, (15-28).

40. A.Murty Kanury, Introduction to Combustion Phenomena

41. Musti, S.. Ignitability of various coals as measured by laser ignition. Master Degree thesis of Chemical engineering department North Carolina A&T State University, 1996.

42. Wall, T. F., Gupta, R. P., Gururajan, V. S., and Zhang, D. The Ignition, buring rate and reacitivity of petroleum coke. Twenty-Third Symposium (International) on Combustion/The Combustion Institute, Pittsburgh, 1990, (1177-1183).